

VILNIUS UNIVERSITY
CENTER FOR PHYSICAL SCIENCES AND
TECHNOLOGY

Kęstutis
IKAMAS

Broadband THz detectors with field effect
transistors: modeling and application
for systems with pulsed and DC sources

SUMMARY OF DOCTORAL DISSERTATION

Technological sciences,
Material engineering **08T**

VILNIUS 2018

The dissertation work was carried out at Vilnius University, Institute of Applied Electrodynamics and Telecommunications from 2014 to 2018.

Scientific supervisor:

Prof. dr. Alvydas Lisauskas (Vilnius University, technological sciences, materials engineering – 08T).

Dissertation will be defended in a public meeting of the Dissertation Defence Panel:

Chairman – Prof. Dr. Vincas Tamošiūnas (Vilnius University, technological sciences, materials engineering – 08T).

Members:

Prof. Dr. Robertas Grigalaitis (Vilnius University, technological sciences, materials engineering – 08T),

Prof. Dr. Artūras Jukna (Vilnius Gediminas Technical University, technological sciences, materials engineering – 08T),

Docent Dr. Dmitry Lyubchenko (KTH Royal Institute of Technology in Stockholm, Sweden, technological sciences, materials engineering – 08T).

Dr. Šarūnas Meškiniš (Kaunas University of Technology, technological sciences, materials engineering – 08T).

The dissertation will be defended at the public meeting of the Dissertation Defence council at 14:30 on 14th of December 2018 in Room D401 of the National Center of Physical and Technological Sciences.

Address: Saulėtekio av. 3, Vilnius, LT-10257, Lithuania.

Tel. +370 5 223 4586; e-mail: kestutis.ikamas@ff.vu.lt

The text of this dissertation can be accessed at the library of Vilnius University, as well as on the website of Vilnius University: www.vu.lt/lt/naujienos/ivykiu-kalendorius.

VILNIAUS UNIVERSITETAS
FIZINIŲ IR TECHNOLOGIJOS MOKSLŲ CENTRAS

Kęstutis
IKAMAS

Plačiajuosčių tranzistorinių THz detektorių
modeliavimas ir taikymas veikai su
impulsiniais ir nuolatinės veikos šaltiniais

DAKTARO DISERTACIJOS SANTRAUKA

Technologijos mokslai,
medžiagų inžinerija **08T**

VILNIUS 2018

Disertacija rengta 2014–2018 metais Vilniaus universiteto Taikomosios elektrodinamikos ir telekomunikacijų institute.

Mokslinis vadovas:

Prof. dr. Alvydas Lisauskas (Vilniaus universitetas, technologijos mokslai, medžiagų inžinerija – 08T).

Gynimo taryba:

Pirmininkas – prof. dr. Vincas Tamošiūnas (Vilniaus universitetas, technologijos mokslai, medžiagų inžinerija – 08T).

Nariai:

prof. dr. Robertas Grigalaitis (Vilniaus universitetas, technologijos mokslai, medžiagų inžinerija – 08T),

prof. dr. Artūras Jukna (Vilniaus Gedimino technikos universitetas, technologijos mokslai, medžiagų inžinerija – 08T),

doc. dr. Dmitry Lyubchenko (KTH karališkasis technologijų institutas, Švedija, technologijos mokslai, medžiagų inžinerija – 08T).

dr. Šarūnas Meškiniš (Kauno technologijos universitetas, technologijos mokslai, medžiagų inžinerija – 08T).

Disertacija bus ginama viešame Gynimo tarybos posėdyje 2018 m. gruodžio mėn. 14 d. 14:30 val. Nacionalinio fizikinių ir technologijos mokslų centro D401 auditorijoje.

Adresas: Saulėtekio al. 3, Vilnius, LT-10257, Lietuva.

Disertaciją galima peržiūrėti Vilniaus universiteto, Fizinių ir technologijos mokslų centro bibliotekose ir VU interneto svetainėje adresu: www.vu.lt/lt/naujienos/ivykiu-kalendorius.

Contents

Introduction	7
Main goal and objectives	9
Scientific novelty	10
Statements to be defended	11
Contribution of the author	13
1 The plasmonic mixing model	14
1.1 Intrinsic responsivity	14
1.2 Detection regimes	15
1.3 The role of gate screening	18
1.4 Chapter summary	18
2 Detector models and simulations	19
2.1 Device responsivity	19
2.2 Antenna EM modeling	22
2.3 Chapter summary	24
3 Broadband Si CMOS 90 nm detectors	26
3.1 Detector designs	26
3.2 Antenna designs	27
3.3 Characterization setups	30
3.4 Characterization results	31
3.5 Chapter summary	34
4 Application of TeraFET for detection of radiation from quantum cascade lasers	35
4.1 The design of detectors	35
4.2 Measurement setups	36
4.3 The comparison of THz detectors performance	38
4.4 A detection of QCL cw radiation	38
4.5 Chapter summary	40
5 Application for linear autocorrelation measurements	41
5.1 AlGaIn/GaN detector	41
5.2 Measurement setup	42

5.3	Linearity of AlGa _N /Ga _N TeraFET response	43
5.4	Linear autocorrelation measurements	43
5.5	Chapter summary	46
6	Investigation of rectification non-linearity in TeraFET detectors	47
6.1	Si and AlGa _N /Ga _N detectors	47
6.2	Measurement setups	49
6.3	Rectification non-linearity in TeraFETs	50
6.4	Nonlinear autocorrelation measurements	52
6.5	Chapter summary	54
	Conclusions	55
	References	57
	List of publications and presentations	64
	List of publications	64
	List of presentations	65
	Santrauka	67
	Curriculum Vitae	68

Introduction

In recent decades, terahertz band of electromagnetic waves (THz) has received much attention. Attempts have been made to use the THz in various fields of science: physics, chemistry, biology, medicine. The THz detectors are anticipated to be useful for defect detection in space vehicles parts, such as telescope antennas, remote detection of explosives at airports, drugs detection and detection of malignant tumors in medicine, quality control systems in the industry and telecommunication [1].

The search for radiation sources and detectors is one of the active THz research areas. Creation of compact broadband and resonant THz detectors continues to be a problem. The biggest demand of such detectors is in mobile THz spectroscopy and space systems, where the small dimensions of THz devices, their durability and the ability to control them are extremely important. The operation of commercial THz detectors available on the market today is based on relatively slow optoacoustic, pyroelectric and bolometer THz detectors, or the ones based on a colorimetric effect at room temperature. The biggest disadvantages of these devices are long response time, low response rates, sensitivity to mechanical and acoustic noise, large dimensions and high costs. Therefore, semiconductor, rectification phenomena-based detectors, such as Schottky diodes or tunnel diodes [2, 3], field-effect transistors (FET) are increasingly becoming a possible alternative. Complementary metal–oxide–semiconductor (CMOS) circuits with FETs and coupled planar antennas (TeraFET) is elegant solution of room temperature THz detector. Detectors of this type are rapidly developing because they can be mass-produced using standard CMOS production technologies [4, 5].

In the last decade of the XX century, Dyakonov and Shur were among the first to suggest using a FET for THz emission detection despite the fact that the signal frequency is larger than cut-off frequency of the

device. They described the response of FET to THz signal as rectified plasma oscillations in the transistor channel [6]. The first FET-based detectors had no built-in antennas and could only detect the powerful THz laser radiation [7, 8]. Over the last few years, TeraFet has improved significantly. The plasmonic-based THz detection principle has been successfully applied to the modeling and simulation of new detectors. Devices with different types of transistors and material systems such as AlGaIn/GaN High Electron Mobility Transistors (HEMT) [9], Si CMOS field-effect transistors [10], nanoscale transistors [11], graphene transistors [12] have been developed. One advantage of Si CMOS TeraFETs [13, 14] is relatively inexpensive technology, which allows creating complex integrated circuits. For example, the Si CMOS TeraFET detectors can be combined into a large array integrating more than one thousand elements [15, 16]. This innovative engineering solution can compete with the commercial focal-plane microbolometers arrays that are currently used in THz image cameras [17].

0.3–10 THz frequency waves can be generated by various types of sources: optoelectronic (photoconductive mixers, non-linear optical crystals), full electronic sources such as multiplication circuits, semiconductor lasers such as quantum cascade lasers, molecular gas lasers, vacuum electronic devices, free electron lasers or gyrotrons. These sources can be the continuous-wave or pulsed ones. Their emission can be sensed by semiconductor detectors in both the homogeneous and heterogeneous modes [18]. However, so far, there are no sensitive Schottky diodes or FET based detectors which can work in a broad frequencies band (span more than 1 THz) – the property which impeded their application in THz spectrometric studies [3].

It is well to bear in mind that it was not the bandwidth of TeraFet that limited the physical rectification process that occurs in the detectors, which basically works effectively in a very wide frequency range [6], but a lack of good design that includes all performance influenced factors

such as loss of power in parasitic elements, or transistor and antenna impedance mismatching [10]. The ability to couple the active element (FET) with the planar antenna and hold the power supply and signal reader electronics in the same Si CMOS chip leads to minimization of the amount of reactive elements and provides a great benefit in developing broadband and sensitive THz detectors.

This dissertation is dedicated to the development peculiarities of broadband transistor-based THz detectors. The investigated physical principles of operation of the devices and applied engineering solutions have allowed the creation of new linear (response is proportional to incident power) detectors that effectively operate in a wide, exceeding three octaves (from 0.25 THz to 2.2 THz) frequency range. The demonstrated responsivity values are at the state-of-the-art level for broadband transistor detectors operating at room-temperature and for this frequency range. The thesis also considers application aspects of the created detectors. The detection of THz waves, radiated by the pulsed and cw sources, with TeraFET has been investigated.

Main goal and objectives

The aim of this dissertation was to create compact broadband sensitive transistor-based detectors optimized for the terahertz frequency band and to study the possibilities of their application.

In order to achieve this goal, the main objectives were defined as follows:

1. To improve the physical model of plasma wave mixing of the field-effect transistor in accordance with the theoretical modeling of the parameters of the high-frequency characteristics of the detector. The difference between the theoretical and experimentally obtained results should not exceed 25 percent.
2. Based on the simulation results, to prepare Si-CMOS detector designs suitable for a THz frequency band with broadband planar

antennas so that foundry can create integrated-circuit chips.

3. To characterize the created Si CMOS THz detectors: determine the main parameters, compare them with those of theoretical models.
4. To study the potential of using Si CMOS and AlGaN/GaN detectors for detection of pulsed and cw radiation emitted by terahertz sources.
5. To study the rectification non-linearity in Si CMOS and AlGaN/GaN THz detectors and the possibility to use this phenomenon for investigation of pulsed terahertz sources.

Scientific novelty

The scientific novelty of the work is based on the following results:

1. The developed analytical model of plasma mixing allows more accurately (with an error of 25 percent or less) to estimate the sensitivity of broadband transistor-based THz detectors at high frequencies, especially those that exceed 1 THz. Another physical model, the accuracy of which is equivalent to that presented, has not yet been described in the literature.
2. The created detector with a bow-tie antenna showed an almost flat response in the frequency range from 0.2 THz to 2.2 THz. Its optical responsivity is 33 mA/W at 609 GHz. The estimated minimum effective noise power (NEP) is $45 \text{ pW}/\sqrt{\text{Hz}}$ at 0.6 THz and $70 \text{ pW}/\sqrt{\text{Hz}}$ at 1.5 THz. The device has no analogues in the field of broadband transistor detectors and even surpasses the best resonant TeraFET detectors in the 1.5 THz frequency range.

3. For the first time, the efficiencies of a transistor THz detector and commercial power THz detectors – the Golay cell and a bolometer — have been compared. Si CMOS transistor-based detectors can detect signals of higher frequency modulation or operate in continuous mode, they can be effectively used as an alternative to traditional THz detectors for monitoring of THz sources, as well as for detection of submicrosecond THz emission processes.
4. It has been found that the response of the AlGaIn/GaN TeraFET is linearly proportional to the radiation power in a broad gate voltage range, even when the device is exposed to THz radiation of up to several hundred milliwatt . It has been shown that transistor detectors can be used for linear autocorrelation measurements and the spectral characterization of pulsed THz sources.
5. Investigation of the non-linear rectification process in Si CMOS and AlGaIn/GaN THz detectors has shown that a super-linear response to the THz radiation power is a universal phenomenon characteristic of all types of FETs. The conditions necessary for its manifestation are as follows: the device shall operate at a voltage below the threshold V_{th} , and the amplitudes of the radiation shall exceed the thermal voltage of transistor but shall not exceed the level at which the saturation mode begins.
6. Nonlinear interferometric autocorrelation studies with a Si CMOS transistor detector have been carried out for the first time. It has been shown that the detector rectification super-linearity can be used to determine and observe the temporal characteristics of THz impulses. The super-linearity of the TeraFET can help measure the speed of the detector internal response.

Statements to be defended

1. In the analytical model of plasma mixing, it is necessary to take into account the loss of power in parasitic elements, channel and antenna impedances mismatching, and the effect of partial shielding of plasmons on the channel impedance. Then, the model will make it possible to better evaluate the responsivity of broadband transistor THz detectors at high frequencies as compared to the other standard models mentioned in the literature or those used in the high-frequency electronics industry, especially when excitation frequencies exceed 1 THz.
2. The improved analytical model, the design of the multilayer planar antenna and the advantages of the Si CMOS technology make it possible to create sensitive broadband transistor-based THz power detectors which are superior to other transistor detectors that have been created using either different design or combination of materials. The created detectors with a bow-tie antenna have a flat responsivity over a frequency range spanning 1.5 THz and a minimum effective noise power of $45 \text{ pW}/\sqrt{\text{Hz}}$.
3. Manufactured Si CMOS detectors which have mass production capabilities and AlGaIn/GaN which has a wide bandgap are suitable for effective monitoring of pulsed and cw THz sources with low and medium power at room temperature. The detectors have high operational flexibility: their response is linearly proportional to the radiation power for a wide range of gate voltages (above the threshold voltage) and for a wide range of source peak powers (from several to several hundred mW).
4. In the strong signal regime, when the THz excitation amplitude at the transistor input exceeds the thermal voltage (at about 10 mV at room temperature), in all transistor-based THz detectors

the super-linearity of the rectification shall be observed. The phenomenon is suitable for detecting and monitoring the temporal characteristics of the ps-long THz pulses using standard techniques such as non-linear interferometric autocorrelation.

Contribution of the author

The author of the dissertation performed part of the work on the development and preparation of the Si CMOS detector design and experimentation methodologies. The author also performed part of the theoretical simulation of Si CMOS and AlGa_N/Ga_N devices using MatLab and Keysight ADS software packages. The author performed almost all the experimental measurements described in the dissertation and contributed to the development of setups, created computer programs for data collection and measurements automation. The author prepared manuscripts of the articles related to the topic of the dissertation and also participated in the preparation of conference presentations, four of which were presented by the author himself.

Part of the results were obtained in collaboration with other laboratories: Ultrafast Spectroscopy and Terahertz-Physics (Institute of Physics, Goethe University, Frankfurt am Main, Germany) led by prof. H. Roskos, Laboratory of Pierre Aigrain (Institute of Ecole Normale Superieure, Paris, France) led by prof. J. Mangeney, Laboratory of THz Spectroscopy of the Institute of Optical Detector Systems of the German Space Center (Berlin, Germany), Laboratory of Ultrafast Optoelectronics (FTMC, Vilnius University, Lithuania) led by prof. A. Krotkus.

1 The plasmonic mixing model

In this work, the theoretical performance parameters of transistor detectors are calculated using a model based on the hydrodynamic equations. The idea of using an FET for detection of THz waves belongs to M. Dyakonov and M. Shur [6]. The detection principle proposed in 1996 is based on the hydrodynamic transport model [19] which considers a two-dimensional electrons gas in the transistor channel considered as a viscous liquid. Incident THz radiation causes collective vibrations of carriers – plasma waves. Detection is possible due to the field transistor non-linear properties that determine the rectification of alternating current generated by the falling THz radiation. As a consequence, the response in the form of DC current or voltage is generated. The signal amplitude is proportional to the radiation power. It is worth noting that the first description of plasma oscillations in 2DEG was given by A. Chaplik in 1972[20].

1.1 Intrinsic responsivity

When the THz signal with voltage amplitude V_a is coupled to the 2DEG in the channel of the FET, it induces voltage response V_{det} . This response can be expressed as the product of a quasi-stationary transistor geometry and material related quantities and a frequency-dependent rectification efficiency factor $f(\omega)$ [10]

$$V_{\text{det}} = \frac{q}{m^*} \frac{V_a^2}{4s^2} \cdot f(\omega), \quad (1)$$

where m^* is the effective mass of electron, q - the elementary charge, ω - the radian frequency of the applied excitation signal and s - the velocity of plasma waves under the gate. The s can be calculated from

the voltage dependency of the resistance (or conductance) of the gated part R_{ch} in the scattering time approximation and for non-degenerate electron gas:

$$s = \sqrt{\frac{q}{m^*} \frac{1}{R_{\text{ch}}} \left(\frac{\partial}{\partial V_{\text{g}}} \frac{1}{R_{\text{ch}}} \right)^{-1}}. \quad (2)$$

The response can also be read out as an induced current signal I_{det} . The I_{det} relates induced voltage through the quasistatic drain-source resistance R_{DC} as $I_{\text{det}} = V_{\text{det}}/R_{\text{DC}}$. The channel with impedance Z_{ch} excited by the amplitude V_{a} will absorb the power.

$$P_{\text{in}} = \frac{V_{\text{a}}^2 \text{Re}(Z_{\text{ch}})}{2 |Z_{\text{ch}}|^2}. \quad (3)$$

The intrinsic responsivity for current \mathfrak{R}_I relates the detector radiation response to this absorbed power:

$$\mathfrak{R}_{I,\text{in}} = \frac{I_{\text{det}}}{P_{\text{in}}} = \frac{q}{2m^*s^2} \cdot \frac{1/R_{\text{ch}}}{\text{Re}(Z_{\text{ch}}^{-1})} \cdot f(\omega). \quad (4)$$

The first term $q/(2m^*s^2)$ in this equation represents the quasistatic responsivity $\mathfrak{R}_{I,\text{QS}}$ of the transistor, the second - the ratio between quasistatic and high-frequency admittances.

1.2 Detection regimes

Plasma oscillations may be formed in fully symmetrically excited FET channels, however no net measurable response to the incident radiation would build up [21]. Efficient rectification can be achieved when one end of the channel (drain or gate) is subject to the full signal oscillation, while the other end (source) is pinned to AC ground. There are two main coupling schemes: the drain-source coupling and the gate-source

coupling. The coupling scheme determines the form of rectification efficiency factor $f(\omega)$.

The propagation and attenuation of the waves in the FET channel is described by two parameters: the complex plasma wavevector k and the length of the gated channel L_g [6]. When frequencies are high ($\omega\tau_p \gg 1$, where τ_p - electron momentum scattering time), the plasma waves can oscillate multiple times before decaying. It is a so-called plasmonic mixing regime. In a short channel ($L_g \leq s\tau_p$), the waves reach the channel end and reflect off the boundary. The channel then acts as a cavity for standing waves and, thus resonance features can evolve. In this case we have a so-called resonant plasmonic mixing regime. When the transistor channel L_g is comparatively long ($L_g \gg s\tau_p$), the waves are overdamped and do not reach the end of the channel. In this device operation regime the factor $f(\omega)$ takes the same form for both coupling schemes:

$$f = 1 + \frac{2\omega\tau_p}{\sqrt{1 + (\omega\tau_p)^2}}. \quad (5)$$

The high-frequency transport in 2DEG can be represented graphically as a RLC transmission line. This line has following elements: resistance $R_i = (qn\mu W)^{-1}$, inductance $L_i = R_i\tau_p$, and the capacitance $C_i = qW\partial n/\partial V_g$ defined per unit of length, where μ - the carrier mobility. This approach can be useful when modeling TeraFET responsivity [4, 22]. An analogy with the RLC line formalism allows representing the FET channel via the lines characteristic impedance $Z_0 = \sqrt{(R_i + i\omega L_i)/(i\omega C_i)}$ and the arbitrary load Z_L :

$$Z_{\text{ch}} = Z_0 \frac{Z_L + Z_0 \tanh(\gamma L_g)}{Z_0 + Z_L \tanh(\gamma L_g)}, \quad (6)$$

where the propagation constant $\gamma = ik^*$.

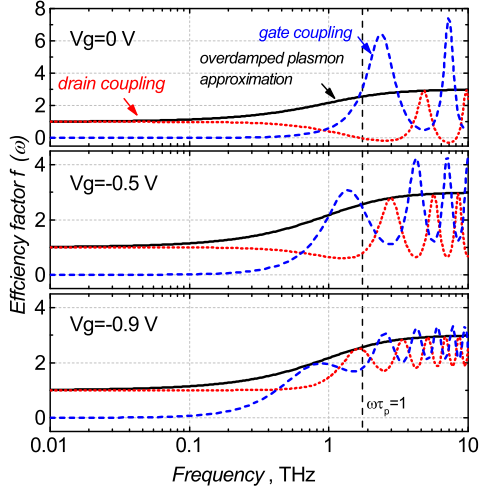


Figure 1: Plasmonic enhancement factors versus radiation frequency for three gate bias voltages V_g . Transistor: AlGaIn/GaN HEMT used in autocorrelation experiments. The red dotted lines denote the enhancement factors for drain coupling, blue dashed lines - for gate-source coupling, and black solid ones - for the overdamped-plasmon limit. [23]

Fig. 1 displays the modeled rectification efficiency factors versus radiation frequency for an AlGaIn/GaN TeraFET. This device was used in the autocorrelation experiments (see chapter 5). Three factors $f(\omega)$ are compared for different coupling schemes. Gate bias voltages used for calculations are 0 V (the FET is normally opened), -0.5 V and -0.95 V (near the threshold voltage). At low frequencies the device operates as a classical resistive mixer. At the frequencies above 100 GHz, this approximation is no longer valid and has to be extended by the non-quasistatic treatment. The overdamped plasmon model gives enhancement (x3) above 1 THz. Fig. 1 also shows the difference between the coupling schemes: the frequencies for the resonance peak depend on the coupling

scheme. The position and height of peaks also depends on the voltage applied to the gate. This feature opens more possibilities to create frequency-agile THz detectors [1, 8, 24]. However this concept does not account for power losses on parasitic elements of device and due to the antenna and channel impedance mismatching, which can diminish the role of plasmonic resonances.

1.3 The role of gate screening

In a standard plasmonic mixing model [6, 10] the plasmons are treated as fully screened by the gate electrode. It is valid if the plasmon wavelength is much longer than the distance d from the channel to the gate electrode ($d \ll 2\pi/\text{Re}(k)$). In the cases, when this condition is not valid, the impedance and the rectification efficiency equations must be revised. The simplest approach is to use transmission line theory formalism. The impedance of the channel equation (6) is needed only for the modification of the capacitance C_i which obtains a more general form $C_i = 2\epsilon_0\bar{\epsilon}W(k + k_s)$ with the effective dielectric constant $\bar{\epsilon}$, the channel width W and the screening wavevector k_s [23]. In this case, the propagation constant is equal to $\gamma = \sqrt{i\omega C_i(R_i + i\omega L_i)}$.

1.4 Chapter summary

This first chapter of thesis presents the plasmonic mixing theory and the transmission line theory, which are the basis of detectors modeling.

2 Detector models and simulations

The model proposed by Dyakonov and Shur prompted the scientists and engineers community to start developing transistor THz detectors and sources. However, the initial plasmonic mixing based rectification theory used many approximations and simplifications of the device design, which hinders the evaluation of the actual performance of THz detectors. For more than 20 years, the FET plasmonic mixing model has been greatly improved. Presented here is the latest model improved by the groups of scientists under the supervision of prof. A. Lisauskas and prof. H. Roskos. [10, 23, 25].

2.1 Device responsivity

The responsivity formula (4) describes the intrinsic detector performance. In reality, any transistor-based device has a number of parasitic elements, such as the capacitance between the gate and source, or the contact resistance, which should be taken into consideration, because they affect device performance, particularly dissipate part of the power entering the detector. In addition, the THz radiation does not come directly into the transistors, but through an antenna located on the same chip. The antenna has its own impedance Z_{ant} , which does not necessarily coincide with the transistor channel impedance Z_{ch} . This impedance mismatching causes an additional loss of power. Thus the device current responsivity can be approximated as follows:

$$\mathfrak{R}_I = \mathfrak{R}_{I,\text{in}} \cdot \eta \cdot M \cdot H_V. \quad (7)$$

The η includes modeled antenna efficiency and optical loss due to reflections and Gaussian beam coupling. The M is a power matching

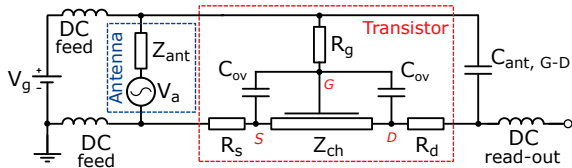


Figure 2: A simplified equivalent circuit of the TeraFET with parasitic elements.[27]

factor. The H_V accounts for the voltage attenuation upon signal transfer from the antenna to the transistor channel.

As long as the FET operates below the limit (f_T), the device can be described in a standard RF electronic circuit model whose component parameters are provided by the foundry for the used technology [26]. However, for higher frequencies, the manufacturer's model, as shown below, may lead to false results. In this paper the analytical physics-based model is used for the description of the device circuit.

The plasmonic mixing based rectification process in the transistor channel can be described as an equivalent DC current (or voltage) source. The simplified equivalent circuit used for modeling of the Si CMOS TeraFET is shown in Fig. 2. The three main parasitic elements are considered in this circuit: the frequency-independent gate and source resistance (respectively, R_{rmG} and R_S) and the high-frequency shunting capacitance $C_{GS,p}$. In this case the mathematical expression of the factor H_V is as follows:

$$H_V = \left| \frac{Z_{ch} \parallel Z_{par}}{Z_{ch} \parallel Z_{par} + Z_{ant} + R_G + R_S} \right|. \quad (8)$$

Here $Z_{ch} \parallel Z_{par}$ denotes the parallel connection of impedances: channel Z_{ch} and shunting capacitance $Z_{par} = (i\omega C_{GS,p})^{-1}$.

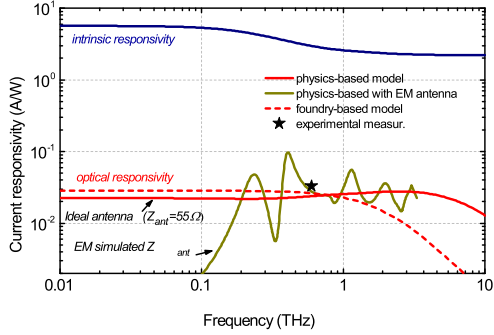


Figure 3: Simulated and measured current responsivity as a function of radiation frequency for the Si CMOS TeraFET. The two models were used: the physics-based (red solid for optical responsivity and dark blue for intrinsic one) and the foundry-based (dashed). The responsivity of a TeraFET with a bow-tie antenna measured at 600 GHz is denoted with a black star. [27]

Another important characteristic which is used for the description of detector performance is effective noise power (NEP). For transistor-based detector without applied drain bias, the main noise source is thermal noise [28]. The NEP of the detector can be derived as

$$NEP = \frac{\sqrt{4k_B T \Delta f}}{\sqrt{R_{DC} \Re_I}} = \frac{\sqrt{4k_B T R_{DC} \Delta f}}{\Re_V}, \quad (9)$$

where Δf denotes the frequency range, which usually equals to 1 Hz.

Fig. 3 shows simulated intrinsic and optical current responsivities versus radiation frequency. Two models were used: foundry-based and physics-based. The gate voltage was 0.45 V (at this point the detector exhibits the best NEP). For simulations a simplified antenna model was used.

This approximation is based on the Babinet principle. For the ideal bow-tie antenna with 90° angle between metal leafs, $Z_{\text{ant}} \approx 100 \Omega$. In addition, a prediction for electromagnetically (EM) simulated frequency-dependent impedance Z_{ant} of the bow-tie antenna is shown (brown line). For frequencies below 1 THz, the responsivities calculated using both models are in a good agreement. However, above 1 THz the physics-based model predicts a slight rise in responsivity, while the foundry-based model predicts a clear roll-off. As shown below (see chapter 3.4), the physics-based device model predicts the performance of a THz detector more accurately than the foundry model.

Fig. 4 shows responsivity simulation results for AlGaIn/GaN HEMT. In this case, an ideal bow-tie antenna with 60° angle between leafs and semi-infinite dielectric with $\epsilon = 9.7$ gives $Z_{\text{ant}} \approx 100 \Omega$. The figure clearly shows that no significant enhancement can be expected in the resonant plasmonic regime. The sharper resonant responsivity spikes can be seen only if the transistor gate voltage is far from the threshold. At this working point the sensitivity of the detector is much lower compared with the optimum sensitivity.

The standard plasmonic mixing or transmission line theory fails to predict frequency roll-off, which is experimentally observed (see Fig. 15(b)). This feature can be explained if the responsivity is calculated including partially gated plasmons (solid curve in the lower part of the Fig. 4).

2.2 Antenna EM modeling

An initial evaluation of the detector sensitivity and the NEP can be done by assuming that the antenna is ideal, i.e. its efficiency and impedance are independent of frequency and equal in fixed values. It is common practice to neglect the antenna electrical properties and

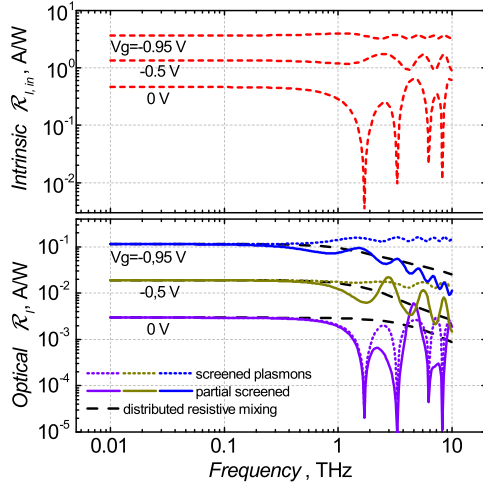


Figure 4: Responsivities versus the radiation frequency of the Al-GaN/GaN TeraFET used in our experiment. The top figure displays the intrinsic responsivity (short-dashed lines) according to eq. (4); the bottom figure displays the optical responsivity calculated using eq. (7) and for three different gate bias voltages V_g . The dotted lines correspond to the case of fully screened plasmons whereas the solid lines account for partial screening and dashed lines correspond to the distributed resistive mixing model. [23]

employ some simplified treatment using either antenna directivity or effective area only. The data obtained demonstrate that it is possible to use consistent physical reasoning and arrive at an accurate estimate of the antenna efficiency, matching and radiation losses. Therefore, even though the antenna model is simplified it serves the purpose of demonstrating impedance matching losses correctly.

Of course, the antenna parameters depend on the frequency and more

precisely, are focused on the optimization of the detector modeling, which should be taken into account. The antenna design was accomplished using electromagnetic simulation tools. In this way all EM aspects of the antenna and the substrate are captured. In this work, for antenna modeling the "Keysight Advanced Design System" was used. This program employs the moments method for EM simulation. Three-dimensional antenna structures were constructed to maximally replicate real structure, including dielectric and metal layers, transmission lines and additional design elements. The analysis, using the moment method, provided information on the main parameters of the antenna: efficiency, directivity, polarization and impedance. The EM simulation results were used for the estimation of the responsivity in the physical model (see brown line in Fig. 3).

THz detectors utilize four types of planar antennas for effective radiation collection: two broadband (bow-tie and log-spiral) and resonant (circular slot with impedance transformation and patch).

2.3 Chapter summary

This chapter presented methods and models for detecting modeling. The analytical physical model developed on the basis of plasmonic mixing theory more accurately describes the THz detector behavior at high frequencies (above 1 THz) and provides more accurate estimates of responsivity, NEP and other device parameters in comparison with those of the standard, foundry-based model. The author is not aware of any other physical approach which could provide results of similar accuracy.

The used model predicts that optical responsivity is significantly lower than the internal sensitivity (20 dB or more) due to impedance mis-

matching between the antenna and the transistor, power losses in parasitic elements of device and optical losses. For correct simulation of TeraFET with a large distance between the gate electrode and the channel ($d > 2\pi/\text{Re}(k)$), it is necessary to include the effect of partial plasmon shielding on the channel impedance in the hydrodynamic transport model.

3 Broadband Si CMOS 90 nm detectors

This chapter presents the development and characterization of broadband Si CMOS 90 nm transistor-based THz detectors. One of the developed TeraFET demonstrated a flat responsivity over a frequency range spanning more than three octaves (from 0.25 THz to 2.2 THz). One possible application of these devices is THz spectrometry.

Most of today's commercial room temperature THz spectrometers are based on semiconductor photomixers, used both as a source and as a detector. Such devices normally operate in a high dynamic range with the homogeneous detection mode [18]. The THz radiation power can also be measured using rectification principle based detectors with Schottky diodes, tunnels diodes [2, 3] or FET detectors [29]. These devices can be used either as direct power meters or adapted for homodyne or heterodyne coherent detection.

3.1 Detector designs

The design of the Si CMOS 90 nm detectors was developed in Cadence Virtuoso Layout Suite environment, the frequently used software package for creation of integrated circuits. All the detectors described in this section are based on one or two ultra low-threshold voltage ($V_{th} \approx 0,48\text{ V}$) NMOS (MOS FET with n-channel). The length of the channel is 100 nm, the width – $1\ \mu\text{m}$. The transistor is connected with a planar antenna using a metallic interconnection (vias). Three variants of the antennas, and, respectively, detectors, were used: a bow-tie, a logarithmic spiral (both are broadband), and a resonant circular slot with an impedance transformation (see 5).

Fig. 6 illustrates the basic layout of the detector. THz radiation enters

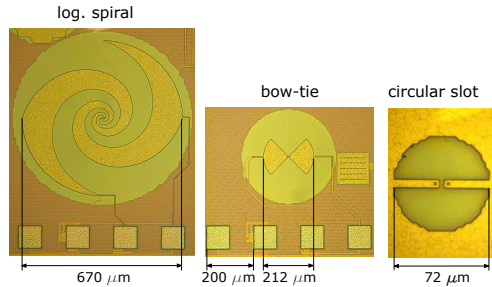


Figure 5: Micrographs of Si CMOS 90 nm TeraFETs with three different antennas.

the antenna from the bottom side through the substrate. The antenna is made of metal and dielectric layers of the CMOS backend. Each antenna leaf consists of two, almost identical shapes, arranged in two metal layers: the thick top and thinner M8. The circuit of connections between the antenna leaves and transistor contacts serves a number of purposes. Firstly, it ensures asymmetric power coupling into the channel from the source side only, which is an essential condition of plasma-wave rectification [6, 10, 13]. Secondly, it ensures independent DC-biasing of the gate and readout of the rectified signal. More details on the design can be found in [27].

3.2 Antenna designs

Si CMOS technology is specially designed to easily integrate into the same miniature chip with a transistor, an antenna and an additional circuit for feeds and read-outs electronics. The antenna is one of the most important elements of the detector. When designing this element it is important that it is not only efficient, but also has an impedance

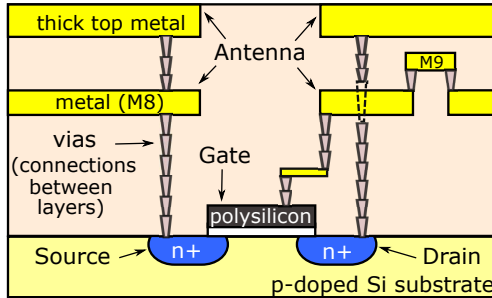


Figure 6: A simplified cross-sectional view of the detector (transistor region). Elements in the view are not to scale. [27]

that is well suited to the load, in our case, the transistor channel.

The parameters of bow-tie antenna were as follows: the angle between the leaves 90° , the length of the leaf $105 \mu\text{m}$, the length of the neck (the gap between the leaves in the middle) $2 \mu\text{m}$. Fig. 5 shows a micrograph image of the antenna and its parasitic circular slot which is required to meet the factory requirements for metal density. At low frequencies ($\sim 150 \text{ GHz}$), the ring absorbs a large amount of THz radiation and dramatically (several dB) reduces the antenna efficiency. The EM modeling of antenna revealed that the bow-tie impedance remains at the same level in a wide frequency range from 0.4 THz to 3.5 THz . The average efficiency is ~ 0.4 . The directivity gradually rises from 8 dBi at 300 GHz to 15 dBi at 2 THz . The results of EM analysis have also shown that the radiation profile becomes more complicated with increasing frequency, and confirms the assumption that the bigger part of EM energy is emitted from the semiconductor substrate rather than the air. The last conclusion justifies why in experiments the THz radiation is directed to the detector from the substrate side.

Another broadband antenna – logarithmic spiral has a 670 μm width, inner radius $r_1 = 17 \mu\text{m}$, the outer radius $r_2 = 27 \mu\text{m}$, the coefficient $a = 0.315$, the number of turns is 1.5. The outer helix radius decreases gradually to r_1 in the last 90 degrees. This ensures a reduction of reflection from the ends of the antenna. As with a bow-tie, a parasitic ring is formed around the spiral. Due to a much larger diameter, the ring effect detector performance below 100 GHz. The EM modeling confirmed that the antenna is broadband: its parameters are relatively flat in the 2 THz frequency range. The imaginary part of the impedance is negative in almost the entire modeled frequency band (from 300 GHz to 2 THz). The antenna performance remains at 0.4 THz to 1.3 THz, and then increases steadily up to 0.8 at 2 THz. The directivity at low frequencies is equal to 8 dBi, but from ~ 600 GHz, it begins to increase steadily to 14 dBi at 2 THz.

The resonant circular slot antenna is formed by two rings: an internal with 36 μm diameter and an external with 148 μm diameter. An impedance transformation dipole is 72 μm long and 6 μm width with 4 μm space between the leaves. EM simulations of structure with such parameters show that its resonant frequency should be at 600 GHz (see Fig. 7). The real detector with circular slot antenna has additional elements which significantly affect the frequency characteristics of the antenna. These elements are CMOS conductors and vias needed to feed the transistor and to connect the antenna to the active element. Upon evaluating their influence, the simulated resonant frequency shifts considerably to lower frequencies (~ 470 GHz). This is confirmed by experimental results (see Fig. 9). The antenna radiation efficiency at 470 GHz is 0.37 and the directivity is 7.2 dBi.

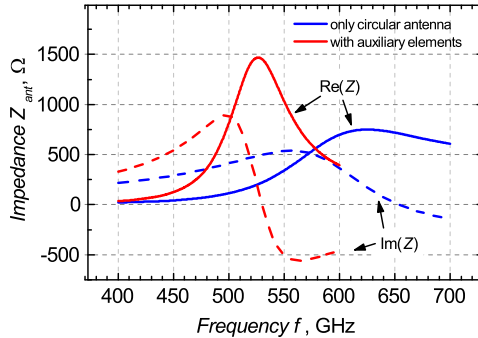


Figure 7: The dependence of the circular slot antenna impedance on the accuracy of the modeling. The continuous line denotes a real part of impedance, the dotted line - an imaginary part. The simulation was done with the Keysight ADS program.

3.3 Characterization setups

TeraFETs were characterized from 0.1 up to 2.2 THz using two THz sources: (a) a tunable multiplier chain-based all-electronic source and (b) a broadband InGaAs photomixer source (TOPTICA TeraScan 1550). The broadband source is based on two temperature-tuned DFB fiber lasers with a 1550 μm center wavelength and can be tuned over a broad frequency range. The available THz power is significantly lower compared to that of the electronic source (respectively, $< 4 \mu\text{W}$ and $60 \mu\text{W}$ at 500 GHz). Due to the sensitivity limitation of the calibrated power meter above 750 GHz, the signal-to-noise ratios (SNR) of TeraFETs and Golay cell were compared to obtain a detector responsivity spectrum.

The Fig. 8 presents a drawing of broadband characterization setup. This setup employs a combination of three off-axis parabolic mirrors of f-number of 2 and a PTFE (Teflon) THz lens for collimation and

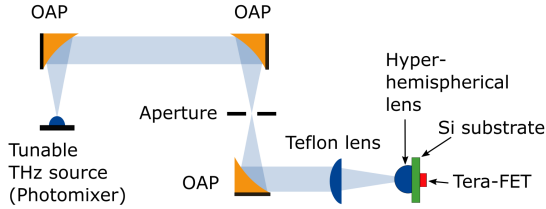


Figure 8: Experimental setup for the TeraFET characterization with a photomixer source for broadband measurements.

focusing of the THz beam. A hyper-hemispherical silicon substrate lens with a 12 mm diameter and a 6.8 mm height in aplanatic optical configuration guided THz radiation into the detector chip. A 7 mm diameter aperture allowed suppressing low-frequency parasitic signals of photomixer source which strongly influenced detector response at frequencies above 1 THz.

3.4 Characterization results

In the setup with a calibrated electronic multiplier-based source the bow-tie TeraFET exhibited a minimum optical (i.e., referenced to the total available beam power) noise equivalent power of $48 \text{ pW}/\sqrt{\text{Hz}}$ and a current responsivity of $33 \text{ mA}/\text{W}$ at 0.6 THz. The log-spiral TeraFET showed a slightly higher NEP of $100 \text{ pW}/\sqrt{\text{Hz}}$, and a responsivity of $11 \text{ mA}/\text{W}$. These measurements are in a good agreement with simulations, which are presented in Fig. 3. The optical performance NEP of the bow-tie detector compares well with sensitivities of TeraFETs in Si CMOS [30] and other technologies such as AlGaN/GaN [9].

The Fig. 9 presents the measured SNR. The measurement was per-

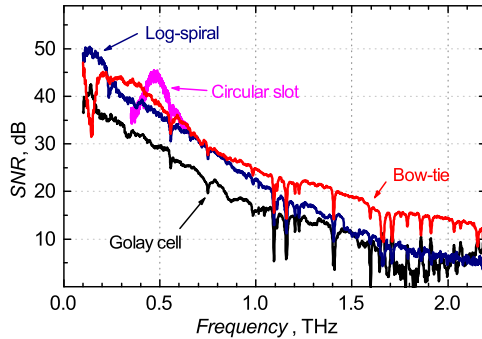


Figure 9: Comparison of the signal-to-noise ratio (SNR) of THz detectors and Golay cell. The gate bias voltage of TeraFET – $V_g = 0.45$ V.[27]

formed with a broadband photomixer source and a lock-in amplifier at a modulation frequency of 888 Hz with a lock-in time constant of 500 ms and at a gate bias voltage of $V_g = 0.45$ V. A nearly linear decrease in the TeraFETs SNR versus frequency is mainly attributed to the decay of the available output power of the photomixer source. In a head-to-head comparison with commercial Golay cell detector, both broadband TeraFETs exceed the dynamic range of the Golay cell by roughly 8 dB.

The Fig. 10 presents the ratio between SNRs of the TeraFET detectors and Golay cell. The Golay cell is assumed to be a flat detector in the measured frequencies range, which lets to conclude on flatness of responsivity spectra of transistor-based detectors. The spectrum of the detector with a bow-tie antenna is almost flat in the 0.2 to 1.75 THz frequency range. Due to the lack of calibrated reference measurement in a higher frequency range, the TeraFET NEP at 1.5 THz is extrapolated from the data of measurements with the multiplier-based source. Given

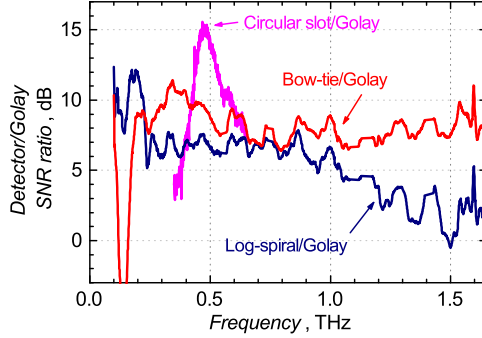


Figure 10: The SNR ratios of the TeraFET and the Golay cell detectors.[27]

the minimum optical NEP of $48 \text{ pW}/\sqrt{\text{Hz}}$ determined at 0.6 THz, one estimates an optical NEP of $70 \text{ pW}/\sqrt{\text{Hz}}$ at 1.5 THz. These values are at the state-of-the-art level for broadband TeraFETs operating at room-temperature and for this frequency range. Moreover, the presented device outperforms the best resonant TeraFet detectors in the 1.5 THz range [15, 29, 31] [30, p. 249].

The detector with a log-spiral antenna showed a narrower region of flat frequency response ($100 \text{ pW}/\sqrt{\text{Hz}}$ at 0.6 THz and 1 THz). Since the ratios for different antenna-coupled TeraFETs show similar spectral modulations, it can be attributed to etalon resonances due to reflections in the diamond window of the Golay cell.

A strong 15 dB dip in the SNR of a bow-tie detector around 150 GHz corresponds to the interaction of the antenna with the surrounding metal which forms a ring (see micrograph in Fig. 5). The log-spiral design does not exhibit this feature because of a wider surrounding ring.

The TeraFET with a narrowband circular slot antenna reaches an optical NEP of $17 \text{ pW}/\sqrt{\text{Hz}}$ at the resonance frequency of 490 GHz. The bandwidth of the detector is ~ 90 GHz, the dynamic range is more than 15 dB higher than the Golay cell and 8 dB higher than the bow-tie TeraFET.

3.5 Chapter summary

Detailed design and characterization of three TeraFET detectors were presented. The two devices are broadband and have an integrated planar antennas: the bow-tie and the logarithmic spiral ones. The third detector is narrowband, its antenna is a circular slot with impedance transformation. Detector performance parameters are successfully optimized during the design development stage using a self-developed physical analytical model and electromagnetic antenna modeling. Improvements in the equipment were also based on the characterization results from previously developed versions of the devices. The results obtained at 1.5 THz for TeraFET with a bow-tie antenna are superior to the best ones reported in the literature for narrowband TeraFETs at this frequency and only up to a factor of four inferior to the results of the best narrowband semiconductor room-temperature devices at 0.6 THz.

4 Application of TeraFET for detection of radiation from quantum cascade lasers

In most practical applications, THz quantum cascade lasers (QCL) are used in conjunction with conventional THz detectors, such as the Golay cell, pyroelectric detector or bolometer. In spite of all these achievements, the demand for sensitive, fast and compact detectors suitable for QCL still remains in the THz range. Only a few reports of attempts to combine TeraFET with THz QCL can be found in the literature [32, 33]. In this chapter, the detection of THz radiation from QCLs using silicon TeraFETs will be considered.

4.1 The design of detectors

For experiments two types of detectors with patch antenna were used. They were designed at the University of Frankfurt (Germany) and were manufactured at two Taiwanese factories: United Microelectronics Corporation (UMC) and Taiwan Semiconductor Manufacturing Company Limited (TSMC). In both cases, the Si 90 nm CMOS technology was used for manufacturing.

UMC TeraFET possesses its best sensitivity at 3.1 THz. The size of the antenna patch is $20.3 \times 20.3 \mu\text{m}$, gate width – 120 nm, impedance at the best sensitivity bias – 14.5 k Ω . The effective area of this antenna assuming the modeled 6 dB directivity is below 100 μm . The Golay cell and bolometer, two other types of the sensors used, had much larger apertures – 6 mm and 15 mm, respectively. The antenna was connected to two NMOS transistors [29].

TSMC chip consists of a dozen FETs with a patch antenna. Each

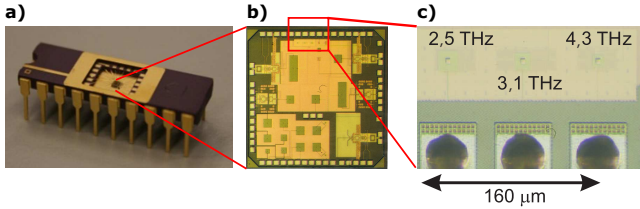


Figure 11: The Si CMOS TeraFET used for the detection of MIT QCL radiation: (a) a standard dual in-line package, (b) a monolithic integrated circuit with many detectors, (c, middle) the micrograph of 3.1 THz detector with a patch antenna.[35]

detector is characterized by different dimensions of the patch, height between the antenna and the ground plane, dimensions of the metallic cup. The resonant frequencies are in the range between 1.35–5.75 THz. Unlike the UMC detector, in the TSMC devices the rectification element consists of only one transistor with the channel length of $L = 100$ nm and a width of $W = 400$ nm [34]. The TeraFET designed for 4.75 THz has dimensions of the antenna of $13 \times 13 \mu\text{m}^2$ and the height to the ground-plane of $2.2 \mu\text{m}$.

4.2 Measurement setups

Three different QCLs were used for two experiments. The first experiment was conducted with one, nominally 3 THz laser which was fabricated at the Massachusetts Institute of Technology (MIT). For the characterizations, the laser was placed into a liquid-helium flow-cycle optical cryostat. The laser was biased with short (down to several hundreds of ns) pulses bundled into trains. A QCL has non-linear IV characteristics, which creates difficulties for impedance matching to a typical 50Ω line. Therefore, in order to avoid voltage spikes special sup-

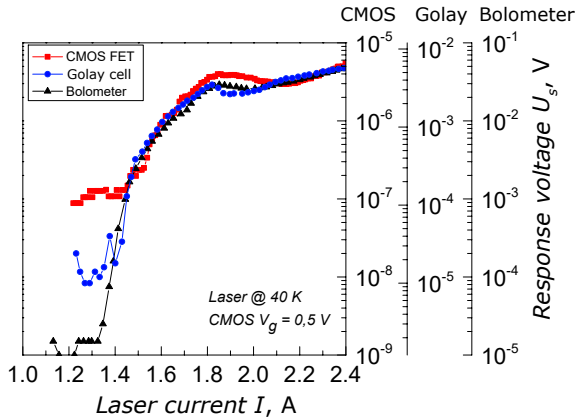


Figure 12: Response voltage V_{det} dependencies on laser current I for three types of detectors: the Si CMOS TeraFET, the Golay cell and the bolometer. [35]

precision of reflections techniques were used, including, a long (75 meters) low-loss 50Ω cable, a 3 dB power absorber and a current doubler [35]. In pulsed operation the maximum operation temperature of the laser reached 165K.

The second experiment was conducted with an LO development platform which is an exact copy of the platform used in the Stratospheric Observatory For Infrared Astronomy (SOFIA) [36]. Two variants of system with, respectively, 4.75 THz and 3.1 THz QCL lasers were used. The devices were produced by the Ferdinand Braun Institute in Berlin. The used cooling system was capable of maintaining the QCL temperature at 49 K. The room-temperature CMOS TeraFET does not need any chopping or other THz signal modulation of the QCL power, therefore the measurements with SOFIA LO were conducted in CW mode at room temperature [34].

4.3 The comparison of THz detectors performance

In the first experiments the performance of three different THz detectors – the TeraFET, the Golay cell and the cryogenic bolometer, were compared. The last two devices are standard commercially available detectors. The results of the experiments are presented in Fig. 12. The laser temperature was fixed at 40 K. The used TeraFET threshold radiation level ($I = 1.4$ A) is slightly higher than that of the Golay cell (1.3 A) or bolometer (1.2 A). In the used optical system Si CMOS TeraFET showed about two rows of dynamic range of responsivity. It is approximately 5 times less than the dynamic range of the Golay cell and about two rows less than the result shown by the bolometer. The previous TeraFET characterization experiment (conducted by the colleagues from Frankfurt University) showed that the device has an NEP of $85 \text{ pW}/\sqrt{\text{Hz}}$ [29]. This value is significantly lower than that of the Golay cell NEP ($\geq 250 \text{ pW}/\sqrt{\text{Hz}}$). Thus, TeraFET could exhibit a higher dynamic range in the case of bigger effective antenna aperture or tighter focusing optics, such as a hyper-hemispherical Si lens or a horn. This assumption is confirmed by the characterization results for the circular slot detector (see sec. 3.4). Based on the above assumptions it may be stated that Si CMOS TeraFETs are suitable for QCL stabilization in various experiments, such as spectroscopy or space exploration. Taking into account inherently faster speed of response, TeraFETs are capable of substituting commercial THz sensors, especially the Golay cells.

4.4 A detection of QCL cw radiation

Eight TeraFET detectors with different resonant frequencies were tested in the SOFIA experiment. The voltage response V_{det} to 4.75 THz QCL

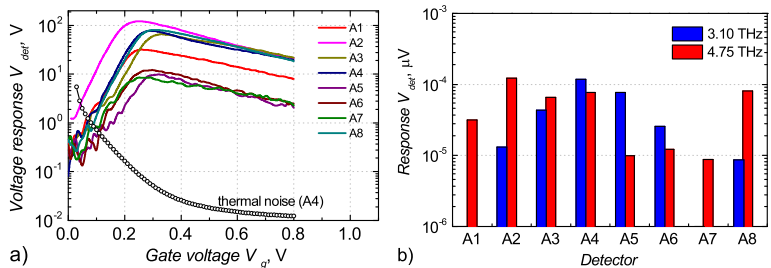


Figure 13: a) The voltage response V_{det} dependence on bias voltage $V_g =$. The QCL frequency – 4.75 THz. The black line with symbols denotes the simulated thermal noise of TeraFET. Tags A1–A8 mark TeraFETs with different antenna design and, respectively, central frequency (from 1.35 THz of A1 to 5.75 THz of A8). b) Response voltages at the maximum of voltage responsivity for TeraFETs to 3.1 THz and 4.75 THz radiation. The performance of devices A1 and A7 was evaluated only with a 4.75 THz laser.

continuous wave radiation are presented in Fig. 13(a). Despite the fact that the majority of detectors had a central frequency of less or more than 4.75 THz, all of them succeeded in detecting QCL radiation. The dynamic range of the responsivity varied from 2.5 dB to 3.5 dB.

Response voltages at the maximum of voltage responsivity for TeraFETs to 3.1 THz and 4.75 THz radiation are presented in Fig. 13(b). The highest response was observed with devices A4 and A2, which have the closest antenna resonance frequencies to those of THz QCLs (3.17 THz and 4.6 THz, respectively). A strong response to 4.75 THz radiation was observed with device A8 with a fundamental resonance at 1.35 THz. This result can be explained by an excitation of higher-order resonance in the patch antenna. The maximum responsivity demonstrated by device A2 was 75 V/W , the minimal NEP – $404 \text{ pW}/\sqrt{\text{Hz}}$ at $V_g = 0.45 \text{ V}$.

These values are at the state-of-the-art level for electronic detectors operating at room-temperature and this frequency range.

The experiment with a SOFIA oscillator results confirmed the assumption that TeraFETs may be used to detect QCL radiation, while the Si CMOS TeraFETs with a patch antenna could be employed for power monitoring of THz QCL used in a spectrometer GREAT.

4.5 Chapter summary

The detection of quantum cascade lasers THz radiation using silicon TeraFETs was presented. The data obtained suggest that Si CMOS TeraFETs are suitable for QCL stabilization in various experiments, such as spectroscopy or space exploration. One TeraFET with patch antenna demonstrated the minimal NEP of $404 \text{ pW}/\sqrt{\text{Hz}}$ and the maximum responsivity of 75 V/W . These values are at the state-of-the-art level for electronic detectors operating at room-temperature and this frequency range.

5 Application for linear autocorrelation measurements

Autocorrelation techniques for short-pulse measurement are applied in a very wide spectrum of electromagnetic waves, including THz frequencies. FET with an integrated planar antenna came into use in THz autocorrelators most recently [37, 38] as an alternative to the Schottky diodes [37]. The autocorrelation curve measured by a linear detector makes it possible to find out the shape and the spectrum of THz pulse of the source. Linear autocorrelation measurements can also be used to investigate the detector itself. The following experimental results revealed the possibilities of TeraFET application in linear autocorrelation systems.

5.1 AlGaIn/GaN detector

A bow-tie antenna coupled THz detector based on AlGaIn/GaN HEMT and a bow-tie antenna were used for linear autocorrelation experiments. The TeraFET employs a single-transistor layout. The transistor gate length is $0.1 \mu\text{m}$, the width – $3 \mu\text{m}$, the distance between the gate electrode and the channel (dielectric layer thickness) – 14 nm . The device was designed at Frankfurt University and fabricated by the GaN MMIC process on the SiC substrate at the Ferdinand Braun Institute (Germany). A hyper-hemispherical silicon substrate lens was used to enhance coupling of THz radiation. More details on the detector concept are given in [9]. The transistor channel is fully open at the zero gate bias and the negative bias voltage is used to control the channel. The following detector parameters were obtained by applying the fitting procedure for quasistatic IV measurements: the threshold voltage was

0.98 V, the electron mobility was $1013 \text{ cm}^2/\text{Vs}$ and the total ungated resistance was 651Ω . A greater part of the resistance (about 550Ω) falls on the ungated access regions of the FET channel.

5.2 Measurement setup

The measurement setup employs a Ti:sapphire laser for generation of infrared radiation pulses with 15-47 fs duration. This setup was part of a THz time domain spectroscopy system (THz-TDS). The laser beam was separated into two optical paths. One of them was delayed with a mechanical stage. Then both arms were guided to a large-area interdigitated low-temperature GaAs photoconductive antenna which generated two independent, identical THz pulses with a variable delay. The power of THz emission was controlled by biasing of the antenna. The average power of terahertz radiation was $15 \mu\text{W}$, the calculated peak power per one pulse was 0.4 W .

The measurable bandwidth of the TDS system can reach up to 14.5 THz with the spectra maximum at approximately 1.5 THz within the dynamic range of 10^3 [39]. The emitted THz radiation was collimated and focused with off-axis parabolic mirrors onto TeraFET. The response of the detector was measured using the lock-in technique. Usual time-domain characterizations using electro-optical (EO) detector (ZnTe crystal) have been performed for the measurement of the bandwidth of the emitted radiation and comparative autocorrelation. A more detailed description of measurement setup is given elsewhere [23].

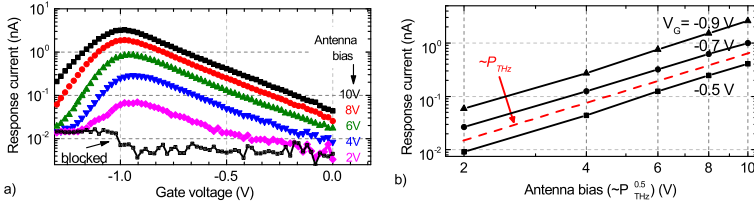


Figure 14: a) The AlGaIn/GaN HEMT current response to the pulsed THz radiation at different intensities and gate biases. b) The vertical cross-sections of the diagram at -0.5 V, -0.7 V and -0.9 V of gate bias voltage. The red line is a guide ($I_{\text{det}} \propto P_{\text{THz}}$) to the eye. [23]

5.3 Linearity of AlGaIn/GaN TeraFET response

Plasmonic mixing in TeraFET theories gives a linear intensity dependence of photoresponse for low power radiation [6, 40, 41]. Pulsed THz sources based on photomixing usually exhibit low average power levels reaching only several μW . However the peak power can be as high as 1 W. Therefore, the investigations of TeraFET began with measurements of the response of AlGaIn/GaN detector versus the power of THz radiation. Fig. 14 shows the results of these measurements. Within the range for which $P_{\text{THz}} \propto I_{\text{ph}}^2$, where I_{ph} is a photo-generated current, it has been found that the detected signal follows the source bias amplitude to the square (see Fig. 19) for a wide range of gate bias (above the threshold voltage). This confirms that TeraFETs operate as linear THz detectors across a large peak power range (up to Watt levels).

5.4 Linear autocorrelation measurements

Fig. 15 presents an autocorrelation trace recorded with AlGaIn/GaN TeraFET at a bias of -0.95 V. Since the pulse is convoluted with itself,

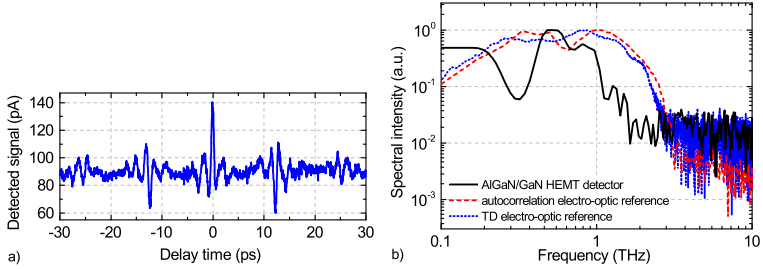


Figure 15: a) Autocorrelation trace of AlGaIn/GaN HEMT response. b) The comparison of spectrum of the response calculated from the autocorrelation trace (solid line), the reference spectra measured with an electro-optic detector in the same setup (dotted line) and the time domain setup (dashed line). The duration of laser pulses is 20 fs, the gate bias voltage of transistor is 0.95 V. [23]

the trace is symmetric. The measured additional peaks with a temporal delay of 12.5 ps cannot be derived from the GaAs antenna spectra. Their origin is the internal reflections in a photomixer emitter. The Fourier transform of the autocorrelation trace (black solid line in Fig. 15 b) contains frequency components from 100 GHz to about 1.5 THz with a signal peak at ~ 580 GHz. A dip at about 300 GHz originates from a metal ring surrounding a bow-tie antenna [9]. The dashed line represents the reference spectrum recorded using the autocorrelation technique, but with a ZnTe crystal as a detector. The dotted line in Fig. 15 b) denotes the spectrum of THz source measured with a probe beam using the time-domain scanning method. The achievable SNR of TeraFET was about 20 dB, whereas a typical SNR for TD-systems is ~ 40 dB. However, the spectral dependencies clearly show that the THz beam contains higher spectral components when recorded with a detector, which allows implementing the pulsed techniques for response bandwidth characterizations. Furthermore, a direct comparison of the SNR values

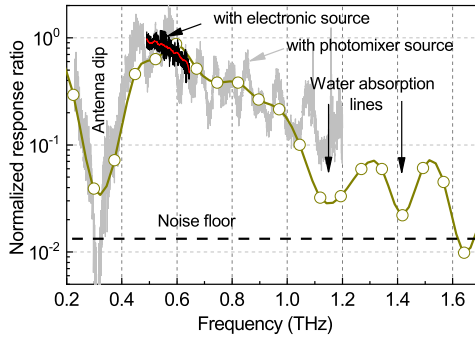


Figure 16: The ratio between the TeraFET response and electro-optic recorded spectra. The red line shows the detector cw characterization with an electronic source, the light gray line in the background denotes the results from photomixer characterizations referenced to the Golay cell detector. [23]

under the same experimental conditions suggests, that TeraFETs can compete with the EO-detectors, and could be used in heterodyne or homodyne configurations.

The linear autocorrelation technique does not allow measuring internal response times for TeraFETs. However, the presence of the non-linear dependency of the response (investigated in more detail in chapter 6) suggests that the response is nearly instantaneous [42] and limited only by the read-out electronics. This statement can be supported by the theory [43] which describes the FET response to short pulses using the viscous hydrodynamic model. Based on this theory, the intrinsic response time for AlGaIn/GaN TeraFET was calculated and is equal to about 50 fs. This value lets speculate that the AlGaIn/GaN TeraFETs can be used in the observation of fast dynamic processes (of at least 1 ps duration) such as the mode-locking processes of the THz QCL.

The general slope of the performance loss over the frequency, clearly visible in Fig. 15 b), was not expected, because the TeraFET was designed to have a nearly flat frequency response up to 1.2 THz. Such behavior is a peculiarity of the device but not the result of the influence of the experimental stand. This assumption was confirmed by another experiment with the same TeraFET but a different photomixer-based system tuneable from 50 GHz to 1.2 THz (Fig. 16). The initial simulation using a standard plasmonic mixing model did not show any roll-off up to 1.2 THz. However, introduction of the partially screened plasmons effect into the model resulted in good agreement between theory and experiment (see Fig. 4).

5.5 Chapter summary

Autocorrelation studies with a broadband AlGa_N/Ga_N TeraFET and a photoconductive antenna excited by fs-long pulses from an infrared laser have shown that the detector can successfully detect THz pulses shorter than the picosecond. The detector response is linearly proportional to the radiated power in a wide peak power range (up to Watt levels). The TeraFET demonstrated SNR (~ 20 dB) lets to conclude that this device could be used in THz autocorrelators as a useful tool for spectral characterization of pulsed THz sources or for a investigation of a detector itself to obtain its temporal characteristics.

6 Investigation of rectification non-linearity in TeraFET detectors

The standard plasmonic mixing in the FET theory states that the TeraFET acts as a linear power detector when the signal is small. When the power of the THz radiation is high, the saturation of response shall be observed. These assumptions are valid for different material systems [44] and for different transistor operating modes (different gate bias voltages) [45, 46]. The saturation phenomenon in the TeraFET detector is applied even to monitor the THz pulse duration using the autocorrelation measurement methods [37].

Recent experiments showed that Si and AlGa_N/Ga_N transistors operating below the threshold voltages and excited by subnanosecond THz pulses, do not behave as the theory predicts – exhibit a super-linear response slope before reaching the saturation [47]. In this regime the voltage signal of a FET is proportional to the radiation power as $V_{\text{det}} \propto P_{\text{THz}}^n$, where the index n is greater than 1.

In this chapter, the super-linear response of FETs is investigated. TeraFET will be considered as a non-linear element which possibly could be applied as a detector for non-linear THz autocorellators.

6.1 Si and AlGa_N/Ga_N detectors

Two broadband detectors with a bow-tie antenna were used to study the rectification non-linearity phenomenon. The first detector – AlGa_N/Ga_N TeraFET is described in sec.5.1. The second detector is Si CMOS 90 nm TeraFET. It is the previous version of the device described in sec. 3.1. Unlike the latest version, the one used for the non-linear

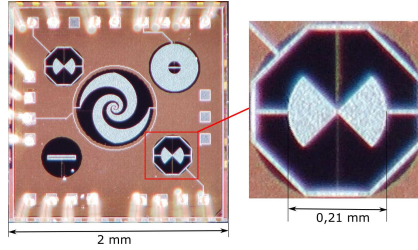


Figure 17: The micrograph image of a Si CMOS crystal with TeraFETs coupled with different antennas. The magnification shows the layout of the bow-tie detector used in this chapter.

regime investigation has two NMOS transistors design [4, 10] with a channel length of 100 nm and a width of 500 nm. Fig. 17 presents the micrograph of the detector. The layout of the antenna is arranged only in the upper metal layer as compared to the two metal layers design of the latest version. The antenna has an opening angle of 90° , the length of each leaf is $105 \mu\text{m}$. The antenna linear polarization axis coincides with the horizontal symmetry axis of the detector. The radiation (with its polarization vector in the paper plane) is coupled from the bottom of the structure through the substrate. The TeraFET works in unbiased drain regime.

The minimum optical NEP of $67 \text{ pW}/\sqrt{\text{Hz}}$ and the responsivity of $\sim 100 \text{ V/W}$ at 0.6 THz were experimentally determined for a Si CMOS TeraFET using an electronic multiplier-chain source. The presented values are the optical ones, i.e., optical losses introduced by a Si lens and coupling of radiation to the integrated antenna were not deducted (which gives higher intrinsic values).

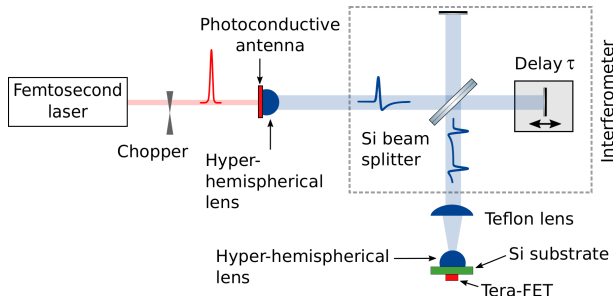


Figure 18: The non-linear THz autocorrelations setup. The power of emitted THz radiation is modulated by biasing a photoconductive antenna emitter with a DC source (not shown on diagram). The response of TeraFET was measured using the lock-in technique (also omitted here). [48]

6.2 Measurement setups

For the investigation of the detector response non-linearity, two THz radiation sources with a photoconductive antenna driven tens-of-femtosecond-long infrared pulses from a Ti:sapphire laser system were employed. The AlGaIn/GaN TeraFET were investigated with the setup which is described in sec. 5.2. The setup dedicated to the Si CMOS TeraFET is shown in Fig. 18. This setup was also used for the non-linear autocorrelation measurements. The GaAs photoconductive THz emitter is illuminated with a trail of femtosecond laser pulses. The generated THz waves were directed to a standard Michelson interferometer which is based on a Si beam splitter, then they were focused onto the TeraFET detector with a PTFE (Teflon) THz lens. A hyper-hemispherical lens was employed to reduce internal reflections inside the substrate of TeraFET. The average power of THz radiation equaled to $1.25 \mu\text{W}$ at the antenna bias voltage of 50 V.

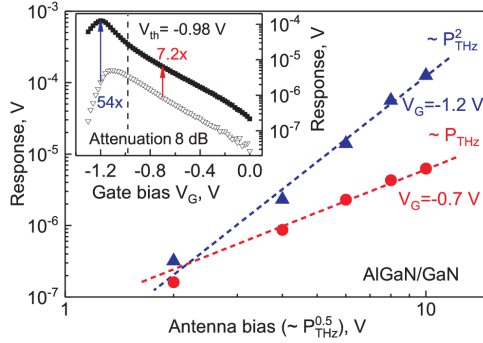


Figure 19: The voltage response of the AlGaIn/GaN TeraFET exposed to pulsed THz radiation for two gate bias voltages: -0.7 V (red dots) and -1.2 V (blue dots). The dashed lines are a guide to the eye. Inset: The response as a function of the FETs gate bias voltage for two THz power levels. The vertical dashed line indicates the turn-on threshold voltage of HEMT. The vertical arrows indicate the enhancement of the voltage response at the given gate bias points when the THz beam power is increased by 8 dB. [42]

6.3 Rectification non-linearity in TeraFETs

The rectification non-linearity in the AlGaIn/GaN detector was investigated using the methodology described in sec. 5.3. When the gate bias voltage was below the threshold (-0.98 V), the detector response dependency on the power became super-linear. Fig. 19 depicts two $V_{\text{det}} = f(P_{\text{THz}})$ dependencies at two bias voltages. At -0.7 V, above the threshold, the curve is linear, but at -1.2 V the dependence becomes almost quadratic. By varying the voltage of the gate, different degrees of dependence can be obtained.

The response of Si CMOS TeraFET versus the power of THz radiation

is presented in Fig. 6.3. These results are in good agreement with the theoretical expectations. In a wide range of gate bias (above the threshold voltage $V_{th} = 445 \text{ mV}$), the response follows antenna bias amplitude to the square. This confirms that TeraFET operates as a linear THz detector across a wide power range. For gate bias below the threshold voltage (at 350 mV and below), the detected signal increases in a super-linear manner. At $V_g = 150 \text{ mV}$, the detected signal is proportional to the third power of the beam intensity or $\sim P^{1.5}$. The deeper into the sub-threshold regime, the steeper the power-vs-response curve becomes. For $V_g = 50 \text{ mV}$, a nearly quadratic dependence ($\sim P^{1.9}$) is observed.

The observed super-linear behavior in AlGaN/GaN HEMT and Si CMOS FET suggests that the phenomenon is universal and it is not dominated by the specific material system. This assumption was confirmed with the help of the device models implementing both the standard non-quasi-static plasmonic mixing model and the distributed transistor model in the "Keysight ADS" software environment. The theoretical analysis has shown that both the super-linear and the saturation regimes of the responsivity are primarily a consequence of the transistor gate voltage dependence of the carrier density in the channel. A super-linear response to high THz intensities was also recently predicted for detectors based on the Schottky diode [49].

Experiments with AlGaN/GaN and Si CMOS TeraFETs confirmed that these detectors employed in setups with a pulsed THz source (a photoconductive antenna) can be a useful tool for investigation of rectification non-linearity phenomenon in transistors. The detector responses are relatively high (dynamic range exceeds 20 dB) even when they are excited with ultrashort THz pulses.

All response regimes of the TeraFET detector were employed in the

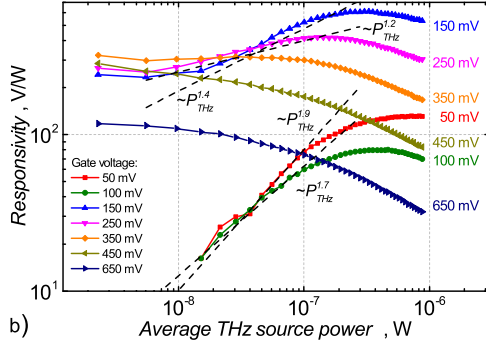


Figure 20: The voltage response of the Si CMOS TeraFET to pulsed THz radiation for different gate bias voltages. The threshold voltage of the transistor is 480 mV. The dashed line is a guide to the eye (a linear law $V_{det} \sim P_{THz}$). [48]

non-linear interferometric autocorrelation measurements.

6.4 Nonlinear autocorrelation measurements

An autocorrelation was performed with a linear detector discards phase information. For determination of the intrinsic response speed of the detector itself, for the measurement of THz pulse duration the non-linear detection process is needed. The interferometric autocorrelation signal recorded by such a detector can be defined by:

$$V_{det}(\tau_p) \propto \int dt \left((E(t) + E(t + \tau_p))^2 \right)^n, \quad (10)$$

here the index $n > 1$. In sub-threshold gate bias regime, the TeraFET can act as a non-linear detector. The deeper into the sub-threshold

regime, the higher number n is (can reach 2 or even larger values). The modulation depth is also larger than 2:1.

Fig. 21 shows autocorrelation interferograms for a Si CMOS TeraFET. The measured curves are normalized to the non-interfering constant value. Above the threshold $V_{th} = 445mV$, where the transistor is in the linear regime, the normalized response does not depend on the gate voltage and overlaps. The modulation depth is 1.5:1. In theory it must be 2:1. The smaller modulation depth could be explained by a non-ideal justification of an interferometer and the beam splitter function influence. Fig. 21 also presents a reference interferogram recorded with the Golay cell (dashed line). This detector presumably was assumed to exhibit a flat frequency response and was expected to demonstrate a near ideal, 2:1 modulation depth in an autocorrelation interferogram. The measured lower modulation depth of 1.7:1 indicated the necessity for improvement of the spectrometer.

When the transistor is in the sub-threshold bias regime, the measured autocorrelation trace exhibits a higher than 2:1 ratio. It indicates a strong non-linear response. The deeper into the sub-threshold regime (lower V_g), the bigger the modulation depth is observed. The maximum depth was 4.5:1 at 50 mV. The n numbers in Fig. 21 indicate the exponent in (10). These values were obtained by fitting Fig. 6.3 curves in the region of powers, where the super-linearity phenomenon manifests itself (between 10 nW and 100 nW). The autocorrelation traces are symmetric, however, they exhibit additional peaks with a temporal delay of 12.5 ps. These peaks originate from the internal reflections in a Si beam splitter (an etalon effect). This phenomenon is a parasitic signal because it obscures some important features of the spectrum.

The proposed detection method is capable of indirectly extracting the THz pulse phase information using a power detector. The observed

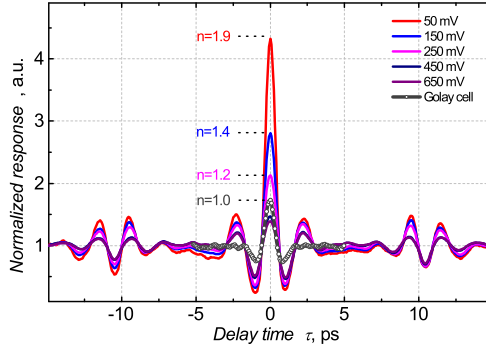


Figure 21: The autocorrelation traces of the Si CMOS TeraFET recorded at different gate-voltages (solid lines). The line with symbols denotes the measurement with the Golay cell. The sub-threshold bias regimes for the TeraFET are below 450 mV. The n numbers indicate the modeled exponent of relation between the detector response and the radiation power. [48]

higher-order non-linear phenomenon could be used as a tool for monitoring the temporal characteristics of THz pulses.

6.5 Chapter summary

It has been shown that the transistor-based detector can operate in the super-linear regime. This transistor phenomenon is universal and not dominated by the specific material system. The proposed detection method using non-linear intensity autocorrelation is capable of indirectly extracting the THz pulse phase information using a power detector.

Conclusions

During the four years of doctoral studies, several types of broadband Si CMOS transistor-based detectors, operating at frequencies higher than 0.1 THz, have been developed, manufactured and tested. The new analytical physical model of the rectification in FET channel based on plasmonic mixing theory has been created. This model allows predicting more accurately the performance of THz detectors based on field-effect transistors in comparison with that of a factory-based model. Thus, the proposed model enables the development of more effective TeraFET in the future. Finally, together with the colleagues from Germany, France and Lithuania, the possibilities of application of Si CMOS and AlGaIn/GaN TeraFETs for monitoring and control of the pulsed and cw sources have been investigated.

To summarize the work, the following conclusions were made:

1. The TeraFET response at higher than 1 THz frequencies can be simulated using a physical analytical plasma mixing model which takes into account the power loss in parasitic elements, the impedance mismatch between the transistor channel and the antenna, and the effect of the partially screened plasmons. These supplements provide a good agreement between the estimated device performance parameters and the experimental ones (an average error is 25 percent), and also explain why no increment in responsivity is observed in the resonant plasma mixing regime of TeraFET.
2. Due to the fast response, small dimensions and the ability to work at room temperature, TeraFETs can be effectively used as an alternative to conventional commercial THz detectors (Golay cell,

- cryogenic bolometer) for monitoring sub-microseconds duration transition processes in THz sources.
3. In the development of broadband transistor-based THz detectors, it is necessary to take into account the phenomenon of plasmons screening and its influence on the channel impedance. For better performance in the THz range frequencies, the distance between the channel and the gate electrode must be reduced to a minimum. This design requirement applies to most material systems and technologies, including AlGa_N/Ga_N HEMTs, Si CMOS FETs, graphene or GaAs FETs.
 4. The AlGa_N/Ga_N and Si CMOS TeraFET responses are linearly proportional to the THz radiation power in a wide range of gate bias voltage, even when the peak power reaches several hundred milliwatts. The demonstrated performance characteristics allow the application of detectors for linear autocorrelation measurements and the spectral characterization of pulsed THz sources.
 5. Super-linear dependence of response to THz radiation power is a universal phenomenon occurring in TeraFET devices. The conditions for the manifestation are as follows: the gate voltage of the device must be lower than the threshold V_{th} , and THz radiation must be less than the values at which the saturation regime begins. The power range, in which super-linear phenomenon is observed, spans less than 10 dB.
 6. The super-linear regime of TeraFET device can be used to determine and monitor the temporal characteristics of THz pulses using non-linear interferometric autocorrelation. These techniques can also be employed for the determination of the intrinsic response time of the FET avoiding limitations set by the read-out electronics.

References

- [1] M. Tonouchi, “Cutting-edge terahertz technology,” *Nature Photonics*, vol. 1, no. 2, pp. 97–105, FEB 2007.
- [2] G. C. Trichopoulos, H. L. Mosbacker, D. Burdette, and K. Sertel, “A broadband focal plane array camera for real-time THz imaging applications,” *IEEE Trans. Antennas Propag.*, vol. 61, no. 4, pp. 1733–1740, Apr. 2013.
- [3] M. Yahyapour, N. Vieweg, A. Roggenbuck, F. Rettich, O. Cojocari, and A. Deninger, “A flexible phase-insensitive system for broadband cw-terahertz spectroscopy and imaging,” *IEEE Trans. Terahertz Sci. Technol.*, vol. 6, no. 5, pp. 670–673, Sept 2016.
- [4] A. Lisauskas, U. Pfeiffer, E. Öjefors, P. Haring Bolívar, D. Glaab, and H. G. Roskos, “Rational design of high-responsivity detectors of terahertz radiation based on distributed self-mixing in silicon field-effect transistors,” *J. Appl. Phys.*, vol. 105, no. 11, p. 114511, Jun 2009.
- [5] F. Schuster, D. Coquillat, H. Videlier, M. Sakowicz, F. Teppe, L. Dussopt, B. Giffard, T. Skotnicki, and W. Knap, “Broadband terahertz imaging with highly sensitive silicon CMOS detectors,” *Opt. Express*, vol. 19, no. 8, pp. 7827–7832, Apr 2011.
- [6] M. Dyakonov and M. Shur, “Detection, mixing, and frequency multiplication of terahertz radiation by two-dimensional electronic fluid,” *IEEE Trans. Electron. Dev.*, vol. 43, no. 3, pp. 380–387, 1996.
- [7] J.-Q. Lu, M. Shur, J. Hesler, L. Sun, and R. Weikle, “Terahertz detector utilizing two-dimensional electronic fluid,” *IEEE Electron Device Lett.*, vol. 19, no. 10, pp. 373–375, Oct. 1998.
- [8] A. El Fatimy, F. Teppe, N. Dyakonova, W. Knap, D. Seliuta, G. Valušis, A. Shchepetov, Y. Roelens, S. Bollaert, A. Cappy, and S. Rumyantsev, “Resonant and voltage-tunable terahertz detection

- in InGaAs/InP nanometer transistors,” *Appl. Phys. Lett.*, vol. 89, no. 13, p. 131926, 2006.
- [9] M. Bauer, A. Ramer, S. Boppel, S. Chevtchenko, A. Lisauskas, W. Heinrich, V. Krozer, and H. G. Roskos, “High-sensitivity wide-band THz detectors based on GaN HEMTs with integrated bow-tie antennas,” in *Proc. 10th European Microwave Integrated Circuits Conference (EuMIC)*. Paris: IEEE, Sep. 2015, pp. 1–4.
- [10] S. Boppel, A. Lisauskas, M. Mundt, D. Seliuta, L. Minkevičius, I. Kašalynas, G. Valušis, M. Mittendorff, S. Winnerl, V. Krozer, and H. G. Roskos, “CMOS integrated antenna-coupled field-effect transistors for the detection of radiation from 0.2 to 4.3 THz,” *IEEE Trans. Microwave Theory Tech.*, vol. 60, no. 12, pp. 3834–3843, Dec. 2012.
- [11] L. Romeo, D. Coquillat, M. Pea, D. Ercolani, F. Beltram, L. Sorba, W. Knap, A. Tredicucci, and M. S. Vitiello, “Nanowire-based field effect transistors for terahertz detection and imaging systems,” *Nanotechnology*, vol. 24, no. 21, p. 214005, May 2013.
- [12] L. Vicarelli, M. S. Vitiello, D. Coquillat, A. Lombardo, A. C. Ferrari, W. Knap, M. Polini, V. Pellegrini, and A. Tredicucci, “Graphene field-effect transistors as room-temperature terahertz detectors,” *Nature Materials*, vol. 11, no. 10, pp. 865–871, OCT 2012.
- [13] W. Knap, M. Dyakonov, D. Coquillat, F. Teppe, N. Dyakonova, J. Łusakowski, K. Karpierz, M. Sakowicz, G. Valusis, D. Seliuta, I. Kasalynas, A. Fatimy, Y. M. Meziani, and T. Otsuji, “Field Effect Transistors for Terahertz Detection: Physics and First Imaging Applications,” *Journal of Infrared, Millimeter, and Terahertz Waves*, Aug. 2009.
- [14] A. Lisauskas, M. Bauer, S. Boppel, M. Mundt, B. Khamaisi, E. Socher, R. Venckevičius, L. Minkevičius, I. Kašalynas, D. Seliuta, G. Valušis, V. Krozer, and H. G. Roskos, “Exploration of Terahertz Imaging with Silicon MOSFETs,” *Journal of Infrared, Millimeter, and Terahertz Waves*, vol. 35, no. 1, pp. 63–80, Jan. 2014.

-
- [15] R. Al Hadi, H. Sherry, J. Grzyb, Y. Zhao, W. Forster, H. M. Keller, A. Cathelin, A. Kaiser, and U. R. Pfeiffer, "A 1 k-Pixel Video Camera for 0.7-1.1 Terahertz Imaging Applications in 65-nm CMOS," *IEEE J. Solid-State Circuits*, vol. 47, no. 12, pp. 2999–3012, Dec. 2012.
- [16] J. Zdanevičius, M. Bauer, S. Boppel, V. Palenskis, A. Lisauskas, V. Krozer, and H. G. Roskos, "Camera for High-Speed THz Imaging," *J. Infrared Millim. Terahertz Waves*, vol. 36, no. 10, pp. 986–997, Oct 2015.
- [17] N. Oda, "Technology trend in real-time, uncooled image sensors for sub-THz and THz wave detection," in *Proceedings of SPIE*, T. George, A. K. Dutta, and M. S. Islam, Eds., May 2016, p. 98362P.
- [18] P. Jepsen, D. Cooke, and M. Koch, "Terahertz spectroscopy and imaging - Modern techniques and applications," *Laser Photonics Rev.*, vol. 5, no. 1, pp. 124–166, Jan. 2011.
- [19] M. Dyakonov and M. Shur, "Shallow water analogy for a ballistic field effect transistor: New mechanism of plasma wave generation by dc current," *Phys. Rev. Lett.*, vol. 71, no. 15, pp. 2465–2468, Oct. 1993.
- [20] A. V. Chaplik, "Possible crystallization of charge carriers in low-density inversion layers," *Sov. Phys. JETP*, vol. 35, p. 395, 1972.
- [21] S. Boppel, M. Ragauskas, A. Hajo, M. Bauer, A. Lisauskas, S. Chevtchenko, A. Rämmer, I. Kašalynas, G. Valušis, H. J. Würfl, W. Heinrich, G. Tränkle, V. Krozer, and H. G. Roskos, "0.25-um GaN TeraFETs Optimized as THz Power Detectors and Intensity-Gradient Sensors," *IEEE Trans. Terahertz Sci. Technol.*, vol. 6, no. 2, pp. 348–350, Mar. 2016.
- [22] M. Sakhno, A. Golenkov, and F. Sizov, "Uncooled detector challenges: Millimeter-wave and terahertz long channel field effect transistor and Schottky barrier diode detectors," *Journal of Applied Physics*, vol. 114, no. 16, p. 164503, Oct. 2013.

- [23] K. Ikamas, A. Lisauskas, S. Massabeau, M. Bauer, M. Burakevič, J. Vyšniauskas, D. Čibiraitė, V. Krozer, A. Rämmer, S. Shevchenko, W. Heinrich, J. Tignon, S. Dhillon, J. Mangeney, and H. G. Roskos, “Sub-picosecond pulsed THz FET detector characterization in plasmonic detection regime based on autocorrelation technique,” *Semiconductor Science and Technology*, 2018.
- [24] W. Knap, Y. Deng, S. Romyantsev, J.-Q. Lü, M. S. Shur, C. A. Saylor, and L. C. Brunel, “Resonant detection of subterahertz radiation by plasma waves in a submicron field-effect transistor,” *Appl. Phys. Lett.*, vol. 80, no. 18, pp. 3433–3435, 2002.
- [25] M. Bauer, “Hydrodynamic modeling and experimental characterization of the plasmonic and thermoelectric terahertz response of field-effect transistors with integrated broadband antennas in Al-GaN/GaN HEMTs and CVD-grown graphene,” Ph.D. dissertation, Johann Wolfgang Goethe-Universität, 2018.
- [26] W. Zhao and Y. Cao, “New Generation of Predictive Technology Model for Sub-45 nm Early Design Exploration,” *IEEE Transactions on Electron Devices*, vol. 53, no. 11, pp. 2816–2823, Nov. 2006.
- [27] K. Ikamas, D. Cibiraite, A. Lisauskas, M. Bauer, V. Krozer, and H. G. Roskos, “Broadband Terahertz Power Detectors based on 90-nm Silicon CMOS Transistors with Flat Responsivity up to 2.2 THz,” *IEEE Electron Device Letters*, pp. 1–1, 2018.
- [28] D. Čibiraitė, M. Bauer, A. Rämmer, S. Chevtchenko, A. Lisauskas, J. Matukas, V. Krozer, W. Heinrich, and H. G. Roskos, “Enhanced performance of algan/gan hemt-based thz detectors at room temperature and at low temperature,” in *Proc. 42nd Int. Conf. on Infrared, Millimeter, and Terahertz Waves (IRMMW-THz)*, Aug 2017, pp. 1–2.
- [29] M. Bauer, R. Venckevičius, I. Kašalynas, S. Boppel, M. Mundt, L. Minkevičius, A. Lisauskas, G. Valušis, V. Krozer, and H. G. Roskos, “Antenna-coupled field-effect transistors for multi-spectral

- terahertz imaging up to 4.25 THz,” *Opt. Express*, vol. 22, no. 16, p. 19235, Aug. 2014.
- [30] G. Carpintero, L. E. García-Muñoz, H. L. Hartnagel, S. Preu, and A. V. Räsänen, Eds., *Semiconductor Terahertz Technology: Devices and Systems at Room Temperature Operation*. Wiley, 2015.
- [31] A. G. Golenkov and F. F. Sizov, “Performance limits of terahertz zero biased rectifying detectors for direct detection,” *Semiconductor Physics Quantum Electronics and Optoelectronics*, vol. 19, no. 2, pp. 129–138, Jul. 2016.
- [32] F. Teppe, C. Consejo, J. Torres, B. Chenaud, P. Solignac, S. Fatholouloumi, Z. Wasilewski, M. Zholudev, N. Dyakonova, D. Coquillat, A. El Fatimy, P. Buzatu, C. Chaubet, and W. Knap, “Terahertz Detection of Quantum Cascade Laser Emission by Plasma Waves in Field Effect Transistors,” *Acta Physica Polonica A*, vol. 120, no. 5, pp. 930–932, Nov. 2011.
- [33] M. Ravaro, M. Locatelli, L. Viti, D. Ercolani, L. Consolino, S. Bartalini, L. Sorba, M. S. Vitiello, and P. De Natale, “Detection of a 2.8 THz quantum cascade laser with a semiconductor nanowire field-effect transistor coupled to a bow-tie antenna,” *Appl. Phys. Lett.*, vol. 104, no. 8, p. 083116, Feb. 2014.
- [34] J. Zdanevicius, D. Čibiraitė, K. Ikamas, M. Bauer, J. Matukas, A. Lisauskas, H. Richter, T. Hagelschuer, K. Victor, H.-W. Hubers, and H. G. Roskos, “TeraFET detector for measuring power fluctuations of 4.75-THz QCL-generated radiation,” *IEEE Trans. Terahertz Sci. Technol.*, atiduotas spaudai.
- [35] K. Ikamas, A. Lisauskas, S. Boppel, Q. Hu, and H. G. Roskos, “Efficient Detection of 3 THz Radiation from Quantum Cascade Laser Using Silicon CMOS Detectors,” *Journal of Infrared, Millimeter, and Terahertz Waves*, vol. 38, no. 10, pp. 1183–1188, Oct. 2017.
- [36] H. Richter, M. Greiner-Bär, S. G. Pavlov, A. D. Semenov, M. Wienold, L. Schrottke, M. Giehler, R. Hey, H. T. Grahn, and H.-W.

- Hübers, “A compact, continuous-wave terahertz source based on a quantum-cascade laser and a miniature cryocooler,” *Optics Express*, vol. 18, no. 10, p. 10177, May 2010.
- [37] S. Preu, M. Mittendorff, S. Winnerl, O. Cojocari, and A. Penirschke, “THz autocorrelators for ps pulse characterization based on schottky diodes and rectifying field-effect transistors,” *IEEE Trans. Terahertz Sci. Technol.*, vol. 5, no. 6, pp. 922–929, Nov. 2015.
- [38] M. Mittendorff, S. Winnerl, J. Kamann, J. Eroms, D. Weiss, H. Schneider, and M. Helm, “Ultrafast graphene-based broadband THz detector,” *Appl. Phys. Lett.*, vol. 103, no. 2, p. 021113, Jul. 2013.
- [39] M. Baillergeau, K. Maussang, T. Nirrengarten, J. Palomo, L. H. Li, E. H. Linfield, A. G. Davies, S. Dhillon, J. Tignon, and J. Mangeney, “Diffraction-limited ultrabroadband terahertz spectroscopy,” *Scientific Reports*, vol. 6, no. 1, Jul. 2016.
- [40] S. Preu, S. Kim, R. Verma, P. G. Burke, M. S. Sherwin, and A. C. Gossard, “An improved model for non-resonant terahertz detection in field-effect transistors,” *J. Appl. Phys.*, vol. 111, no. 2, p. 024502, 2012.
- [41] A. Lisauskas, M. Bauer, A. Rämmer, K. Ikamas, J. Matukas, S. Chevtchenko, W. Heinrich, V. Krozer, and H. G. Roskos, “Terahertz rectification by plasmons and hot carriers in gated 2D electron gases,” in *Proc. 41st Int. Conf. Noise and Fluctuations (ICNF)*. IEEE, Jun 2015, pp. 1–5.
- [42] A. Lisauskas, K. Ikamas, S. Massabeau, M. Bauer, D. Čibiraitė, J. Matukas, J. Mangeney, M. Mittendorff, S. Winnerl, V. Krozer, and H. G. Roskos, “Field-effect transistors as electrically controllable nonlinear rectifiers for the characterization of terahertz pulses,” *APL Photonics*, vol. 3, no. 5, p. 051705, Mar. 2018.
- [43] S. Rudin, G. Rupper, and M. Shur, “Ultimate response time of high electron mobility transistors,” *Journal of Applied Physics*, vol. 117, no. 17, p. 174502, May 2015.

- [44] D. B. But, C. Drexler, M. V. Sakhno, N. Dyakonova, O. Drachenko, F. F. Sizov, A. Gutin, S. D. Ganichev, and W. Knap, “Nonlinear photoresponse of field effect transistors terahertz detectors at high irradiation intensities,” *J. Appl. Phys.*, vol. 115, no. 16, p. 164514, Apr. 2014.
- [45] A. Gutin, V. Kachorovskii, A. Muraviev, and M. Shur, “Plasmonic terahertz detector response at high intensities,” *J. Appl. Phys.*, vol. 112, no. 1, p. 014508, Jul. 2012.
- [46] S. Rudin, G. Rupper, A. Gutin, and M. Shur, “Theory and measurement of plasmonic terahertz detector response to large signals,” *J. Appl. Phys.*, vol. 115, no. 6, p. 064503, Feb. 2014.
- [47] N. Dyakonova, P. Faltermeier, D. B. But, D. Coquillat, S. D. Ganichev, W. Knap, K. Szkudlarek, and G. Cywinski, “Saturation of photoresponse to intense THz radiation in AlGaIn/GaN HEMT detector,” *J. Appl. Phys.*, vol. 120, no. 16, p. 164507, Oct 2016.
- [48] K. Ikamas, I. Nevinskas, A. Krotkus, and A. Lisauskas, “Silicon field effect transistor as the nonlinear detector for terahertz autocorellators,” 2018, unpublished.
- [49] E. R. Brown, S. Sung, W. S. Grundfest, and Z. D. Taylor, “THz impulse radar for biomedical sensing: nonlinear system behavior,” *Proc. SPIE*, vol. 8941, p. 89411E, Mar. 2014.

List of publications and presentations

List of publications

The list of peer reviewed publications in "Clarivate Analytics Web of Science" journals:

1. K. Ikamas, A. Lisauskas, S. Boppel, Q. Hu, and H. G. Roskos, "Efficient Detection of 3 THz Radiation from Quantum Cascade Laser Using Silicon CMOS Detectors," *J. Infrared Millim. Terahertz Waves*, vol. 38, no. 10, pp. 1183–1188, Oct. 2017.
2. A. Lisauskas, K. Ikamas, S. Massabeau, M. Bauer, D. Čibiraitė, J. Matukas, J. Mangeney, M. Mittendorff, S. Winnerl, V. Krozer, and H. G. Roskos, "Field-effect transistors as electrically controllable nonlinear rectifiers for the characterization of terahertz pulses," *APL Photonics*, vol. 3, no. 5, p. 051705, Mar. 2018.
3. K. Ikamas, D. Čibiraitė, A. Lisauskas, M. Bauer, V. Krozer, and H. G. Roskos, "Terahertz Power Detectors based on 90-nm Silicon CMOS Transistors with over Six Octaves Flat Responsivity," *IEEE Electron Device Lett.*, vol. 39, no. 9, p. 1413–1416, Sep. 2018.

Peer reviewed conference publications:

4. A. Lisauskas, M. Bauer, A. Rämmer, K. Ikamas, J. Matukas, S. Chevtchenko, W. Heinrich, V. Krozer, and H. G. Roskos, "Terahertz rectification by plasmons and hot carriers in gated 2d electron gases," in *Proc. 41st Int. Conf. Noise and Fluctuations (ICNF)*. IEEE, Jun 2015, pp. 1–5.
5. K. Ikamas, A. Lisauskas, M. Bauer, A. Ramer, S. Massabeau, D. Cibiraite, M. Burakevic, S. Chevtchenko, J. Mangeney, W. Heinrich, V. Krozer, and H. G. Roskos, "Efficient detection of short-pulse THz radiation with field effect transistors." in *Proc. 42nd Int. Conf. Noise and Fluctuations (ICNF)*. IEEE, Jun. 2017, pp. 1–4.
6. J. Zdanevicius, K. Ikamas, J. Matukas, A. Lisauskas, H. Richter, H.-W. Hubers, M. Bauer, and H. G. Roskos, "TeraFET detector

for measuring power fluctuations of 4.75-THz QCL-generated radiation.” in *Proc. 42nd Int. Conf. Noise and Fluctuations (ICNF)*. IEEE, Jun. 2017, pp. 1–4.

List of presentations

Presentations at the conferences (underlined K. Ikamas. – presented personally):

1. K. Ikamas, A. Lisauskas, S. Boppel, Q. Hu, and H. G. Roskos, “Terahercinio kvantinio pakopinio lazerio spinduliuotės detekcija silicio CMOS detektoriais”. 41st Lithuanian National Conference of Physics (LNFK), Vilnius, 2015, *postal*.
2. A. Lisauskas, M. Bauer, A. Rämmer, K. Ikamas, J. Matukas, S. Chevtchenko, W. Heinrich, V. Krozer, and H. G. Roskos, “Terahertz rectification by plasmons and hot carriers in gated 2D electron gases,” 41st Int. Conf. Noise and Fluctuations (ICNF), Xi’an, P.R. China, *oral*.
3. K. Ikamas, A. Lisauskas, D. Voß, and H. G. Roskos, “Didelio jautrio plačiajuostis terahercinis silicio KMOP technologijos detektorius”. 42nd Lithuanian National Conference of Physics, Vilnius, 2017, *oral*.
4. K. Ikamas, A. Lisauskas, M. Bauer, A. Ramer, S. Massabeau, D. Cibiraite, M. Burakevic, S. Chevtchenko, J. Mangeney, W. Heinrich, V. Krozer, and H. G. Roskos, “Efficient detection of short-pulse THz radiation with field effect transistors.” International Conference on Noise and Fluctuations (ICNF), Vilnius, 2017, *oral*.
5. J. Zdanevicius, K. Ikamas, J. Matukas, A. Lisauskas, H. Richter, H.-W. Hubers, M. Bauer, and H. G. Roskos, “TeraFET detector for measuring power fluctuations of 4.75-THz QCL-generated radiation.” International Conference on Noise and Fluctuations (ICNF), Vilnius, 2017, *oral*.
6. A. Lisauskas, M. Bauer, K. Ikamas, J. Zdanevicius, D. Voß, D. Čibiraitė, V. Krozer, and H. G. Roskos, “High-performance

- THz detectors in 90 nm Si CMOS technology”. 9th THz Days, Dunkerque, France, 2017, *oral*.
7. K. Ikamas, J. Zdanevicius, L. Dundulis, S. Pralgauskaitė, A. Lisauskas, D. Čibiraitė, D. Voß, V. Krozer, and H. G. Roskos, “Quasi optical THz detectors in Si CMOS.” 22nd International Microwave and Radar Conference (MIKON), Poznan, 2018, *oral*.
 8. S. Pralgauskaitė, K. Ikamas, J. Matukas, A. Lisauskas, V. Jakštas, V. Janonis, I. Kašalynas, P. Prystawko, and M. Leszczynski, “Carrier trapping in the terahertz bow-tie diode based on AlGa_N/Ga_N heterostructures.” 22nd International Microwave and Radar Conference (MIKON), Poznan, 2018, *oral*.
 9. K. Ikamas, D. Čibiraitė, A. Lisauskas, M. Bauer, V. Krozer, and H. G. Roskos, “Ultrabroadband Terahertz Power Detectors based on 90-nm Silicon CMOS Transistors”. 43 International Conference on Infrared, Millimeter and Terahertz Waves, Nagoya, Japan, 2018, *oral*.
 10. H. G. Roskos, M. Bauer, K. Ikamas, F. Ludwig, and A. Lisauskas, “THz Detection With Field-effect Transistors: The Role Of Plasma Waves And Of Thermoelectric Contributions”. 43 International Conference on Infrared, Millimeter and Terahertz Waves, Nagoya, Japan, 2018, *oral*.

Santrauka

Ši disertacija skirta plačiajuosčių tranzistorinių THz detektorių (TeraFET) kūrimo ypatumams. Nagrinėti fizikiniai įrenginių veikimo principai ir inžineriniai sprendimai leido sukurti naujus tiesinius (atsakas tiesiogiai proporcingas spinduliuotės galiai) detektorius, kurie efektyviai veikia plačiame, daugiau nei tris oktavas (nuo 0,25 THz iki 2,2 THz) apimančiame dažnių intervale. Gauti eksperimentuose jautriai nenusileidžia geriausiems šiai dienai plačiajuosčiams tranzistoriniams detektoriams ir nedaug nusileidžia atrankiesiems THz tranzistoriniams detektoriams. Darbe taip pat nagrinėjami taikomieji sukurtų detektorių aspektai: iširtos impulsinių ir nuolatinės veikos šaltinių skleidžiamos THz spinduliuotės detekcijos su TeraFET galimybės. Pirmą kartą tiesiogiai palygintas tranzistorinio THz detektoriaus ir komercinių tiesinių THz detektorių – Golėjaus narvelio ir bolometro, veikos efektyvumas.

Si ir AlGaIn/GaN tranzistorinių detektorių lyginimo netiesiškumų tyrimais įrodyta, kad netiesinė, aukštesnio už vieną laipsnio, atsako priklausomybė nuo THz spinduliuotės galios – universalus, tranzistoriniams detektoriams būdingas reiškinys. Pirmą kartą atlikti su Si tranzistoriniu detektoriumi netiesinės interferometrinės autokoreliacijos tyrimai. Parodyta, kad detektoriaus lyginimo netiesiškumas gali būti panaudotas laikinėms THz impulsų charakteristikoms nustatyti ir stebėti.

Curriculum Vitae

Name, surname: Kęstutis Ikamas
Date of birth: 12/24/1971
Place of birth: Saint Petersburg, Russia
Phone and email: +370 5 223 4586, kestutis.ikamas@ff.vu.lt

Education **2014-2018**
Doctoral studies, Technological sciences
Vilnius University, Physics faculty
1990-1995
B.A. and M.A., Physics
Vilnius University, Physics faculty
1979-1990
secondary education
Vilnius 43 Secondary School

**Scientific
experience** **2014-2018**
junior-researcher
Vilnius University, Physics faculty

Teaching **2015-till now**
lecturer
Vilnius University, Physics faculty
2012-till now
lecturer
Lithuanian Military Academy

Specialization CMOS THz detectors, THz imaging,
their implementation for THz applications;
cybersecurity, ITT technologies

UŽRAŠAMS

Vilniaus universiteto leidykla
Universiteto g. 1, LT-01513 Vilnius
El. p. info@leidykla.vu.lt,
www.leidykla.vu.lt
Tiražas 33 egz.